Condensed title: Mud blisters in oysters

Dynamics of mud blister worm infestation and shell repair by oysters

Kelly M. Dorgan[1,2*], Rachel D. Moseley[1,3], Ellen Titus[1,4], Harrison Watson[1], Sarah M. Cole[1,2], William Walton[1,5]

[1] Dauphin Island Sea Lab, 101 Bienville Blvd, Dauphin Island, AL 36528

[2] University of South Alabama, Department of Marine Sciences, Mobile, AL 36688

[3] Present address: Gulf Coast Research Laboratory, University of Southern Mississippi, Ocean Springs, MS 39564

[4] Present address: East Carolina University, Howell Science Complex, Greenville, NC 27858

[5] Auburn University, AUSL, 150 Agassiz Street, Dauphin Island, AL, 36528

*author for correspondence kdorgan@disl.org

Key words: *Polydora websteri*, biofouling, oyster aquaculture, *Crassostrea virginica*, mud blister breaking force, burrows

ABSTRACT

Mudblister worms bore into oyster shells, and oysters respond to shell penetration by secreting new layers of shell, resulting in mud blisters on inner surfaces of oyster shells. We conducted two experiments in off-bottom oyster farms along Alabama's coast in summer, 2017, to explore the dynamics of worm infestation, blister formation and shell repair. Results support our hypothesis that only a small proportion of worms that bore into oysters create blisters. Triploid oysters had fewer blisters than diploids, likely because of faster growth and recovery. We treated oysters to remove mudblister worms, redeployed them at intertidal and subtidal sites for nine weeks and found that reinfestation by worms occurred only in subtidal oysters. Intertidally deployed oysters showed no visible blister recovery, whereas blister coverage increased in subtidal oysters. Reinfestation of subtidal oysters was correlated with previous burrow damage, visualized with X-ray images, which supported our hypothesis that worms preferentially settle in previously infested shells. Forces required to break blisters, measured with a custom-built shucking knife with integrated force sensor, were low relative to forces required to shuck oysters, possibly because our experiment was conducted when worm infestation was increasing. Higher forces were required to break smaller, lighter-colored blisters, consistent with blister recovery, but results were highly variable and not consistent across sites and sampling times, suggesting that size and color of blisters alone did not explain shell strength. Our results indicate that oysters repair shells slowly relative to more dynamic patterns of worm infestation.

INTRODUCTION

Mudblister worms are spionid polychaetes, e.g., *Polydora websteri*, that settle on and bore into mollusc shells (Blake and Evans, 1973). The mudblister worms can settle in crevices

on the shell surface and secrete an acidic mucous, which dissolves the organic matrices between shell units (Haigler, 1969; Zottoli and Carriker, 1974). Burrows start as shallow grooves, then are deepened to U-shaped burrows (Hopkins 1958). The worm lines its U-shaped tube with detritus that it collects with its palps (Zottoli and Carriker, 1974). When the burrow penetrates through to the inside of the shell, this can irritate the mollusc, prompting it to secrete a thin layer of shell over the burrow creating a mudblister (Haigler, 1969; Bailey-Brock and Ringwood, 1982). Some blisters extend to the periphery of the shell, often with the U-shaped burrow visible through the inner layer of shell, whereas others do not (Handley and Bergquist, 1997). Lunz (1941) suggests that late-stage larvae of *Polydora ciliata* can enter the mantle cavity and settle on the inner layer of the shell, often near the mantle edge (Lunz, 1941). Alternately, these peripheral burrows (e.g., Fig. 1 from Morse et al. 2015) may result from boring through the thin outer margin of the shell (Hopkins 1958). The dynamics of blister formation and subsequent shell repair result from complex interactions between the worms and their mollusc hosts. This study aims to better understand shell recovery from mud blister worm infestation, specifically how shell repair depends on the oyster growth rate and how worm reinfestation drives new blister formation. We focus on eastern oysters, *Crassostrea virginica*, grown in aquaculture, both for ease of sampling and because mudblister worms are a growing concern for oyster aquaculture and are well studied in this system (Bailey-Brock and Ringwood, 1982, Watson et al. 2009, Simon and Sato-Okoshi 2015, Morse et al. 2015, Martinelli et al. 2020).

Whether burrows are created near the periphery or interior of the shell, as described above, is potentially important in determining to what extent worm infestation translates to blister damage. If every worm that settles on the shell causes blister formation, which is more likely if worms settle near the shell margin, then worm abundance will be strongly correlated

65 with blister damage. On the other hand, if not all burrows that begin on the outside of the shell
66 reach deep enough to irritate the oyster, correlation between blisters and burrows will be weak.
67 Previous studies have found more worms than blisters on the shell (Handley and Bergquist 1997,
68 Cole et al. 2020), indicating that not every worm creates a blister. We hypothesize that only a
69 small proportion of worms cause blisters, so worm abundances will be much higher than blister
70 numbers and these variables will not be strongly correlated (H1). In addition to the proportion of
71 worms that initially create blisters, this relationship will depend on how quickly oysters repair
72 their shells versus how long worms live in oysters. Differences in these timescales would likely
73 weaken the correlation between worm abundance and blisters.
74 Once blisters are formed, how quickly oysters repair their shell likely depends on how
75 quickly oysters can grow and secrete new shell layers versus how quickly worms can expand
76 existing blisters or create new blisters. Triploid oysters, used in aquaculture, have 3 sets of
77 chromosomes, making them sterile, and often have higher growth rates than diploids (Walton *et*
78 *al.*, 2013; Stone *et al.*, 2013, Cole et al. 2020). Oyster farmers along the Alabama coast have
79 observed more blister damage in diploid than triploid oysters (W.W., pers. comm.), but we found
80 in a previous study that the abundance of mud blister worms did not differ between triploid and
81 diploid oysters across four sites along the Alabama coast (Cole et al. 2020). This discrepancy
82 could be explained by higher growth rates of triploids: we hypothesize that triploid oysters
83 recover from mudblister damage by laying down shell layers more quickly than diploids, and
84 therefore have fewer, smaller blisters that require larger forces to break (H2). Alternatively,
85 differences in growth rates may not lead to differences in blister damage if worm infestation
86 rates are high and enough new blisters are being formed. Oysters deployed intertidally
87 experience daily air exposure, which has been shown to decrease worm infestation as the worms

88 are unable to tolerate desiccation (Handley and Bergquist, 1997; Simon and Sato-Okoshi, 2015;
89 Gamble, 2016). We hypothesized that blister recovery would be greater in oysters (first treated to
90 remove mud blister worms) deployed intertidally than those deployed subtidally because worm
91 reinfestation would be lower (H3a). Simon et al. (2006) suggested that burrows made by other
92 species of mud blister worms may provide habitat for settling *Boccardia* sp. larvae, and we
93 found that reinfestation was higher in previously infested than previously uninfested shell,
94 although only at a site with intermediate infestation (Cole et al., 2020). In addition to burrows
95 facilitating recruitment, survival of recently settled worms may also be higher when worms settle
96 in existing burrows because they have to exert less energy to create burrow space and have
97 immediate protection. Therefore, we also hypothesized that previous infestation facilitates
98 reinfestation by providing burrow structures for larval worms to settle (H3b).
99 A challenge in assessing oyster recovery from mud blister damage is the ability to
100 distinguish between newly formed blisters and more advanced, "recovered" blisters. Handley
101 and Bergquist (1997) characterized blisters in *C. gigas* from New Zealand as either "new," which
102 were darker in color, covered by a thin nacreous layer, and contained juvenile *Polydora websteri*,
103 or "old," covered by a lighter-colored, thicker layer of shell and containing adult worms. This
104 suggests that as oysters secrete new layers of shell over blisters, the color of the blister becomes
105 lighter, the visible blister becomes smaller, and the strength of the overlying shell increases. We
106 hypothesize that blisters that are lighter in color will require more force to break (H4a) and that
107 larger blisters will break more easily (under smaller forces) than smaller blisters (H4b). Although
108 studies have shown that burrow damage weakens shells to compressive stress (e.g., crushing by
109 decapod claws) (Bergman et al. 1982), we know of no other studies that have measured blister
110 breaking forces. This relationship could potentially be complicated by the timing and amount of

sediment packed into burrows by worms, potential recruitment and movement of worms into existing mud blister burrows and overlapping burrows and blisters. These hypotheses are interdependent and challenging to test in isolation because the dynamics of blister formation and recovery depend on worm recruitment and growth patterns, how recruitment translates to blister damage on the mollusc, and how quickly and effectively the mollusc responds to blister damage, all of which are difficult to measure as quantifying blisters requires destructive sampling of molluscan hosts. Finally, in this study, we aim to develop better methods for assessing recovery from blister damage and to better understand which of these driving factors are most important in determining blister damage and recovery.

METHODS

We explored the dynamics of mud blister formation and oyster shell repair by sampling diploid and triploid oysters at three farms on the Alabama coast (Exp. 1) and removing mudblister worms and re-deploying oysters under two environmental treatments (Exp. 2). Worms found in oysters from all three farms were identified as *Polydora websteri* based on morphological examination of live animals (Hopkins et al. 1989; Radashevsky 1999). Our identification was consistent with findings by Rice et al. (2018) that *P. websteri* from the Alabama coast are genetically similar to those from the US East coast, Hawaii, and China. Specimens collected from Dauphin Island are vouchered at the Auburn University Museum of Natural History (AUMNH-45710 to AUMNH-45713). In addition, the COI sequence (GenBank MW270169) matches that of *P. websteri*. We did not closely examine all worms extracted, however, and cannot discount the possibility that other species in the *Polydora* complex were present as well (cf., Simon and Sato-Okoshi, 2015).

134

135 *Experiment 1: Blister occurrence and breaking forces*

136 To relate worm abundance to blister coverage (H1), determine if triploids recover more
137 quickly than diploids (H2), and to measure blister breaking forces (H4), we collected oysters that
138 were originally deployed as spat at three farms on the Alabama coast (Fig. 1). Juvenile oysters
139 (or 'seed') were obtained from the Auburn University Shellfish Laboratory, and oysters were
140 grown in OysterGro™ floating cages containing mesh bags of oysters at three commercial oyster
141 farm sites: Point aux Pins (PAP), Massacre Island (MI) and Navy Cove (NC) (Fig. 1). Sampling
142 for this experiment occurred once oysters had reached near-harvestable size (~75 mm). At each
143 of the three farms, there were 16 bags containing ~50 oysters each (8 bags of each ploidy).
144 Oysters were collected on June 1, June 19, and July 11, 2017. Some mortality of triploid oysters
145 was observed at Navy Cove during the last sampling date, likely caused by a low salinity event
146 (Cole et al. 2020), but live oysters were selected for analysis. On each sampling date, 2 oysters
147 from each bag were collected to generate a sample with a total of 16 oysters of each ploidy from
148 each site. Oysters were transported on ice back to the lab. Twelve of the 16 oysters of each
149 ploidy were haphazardly chosen for analysis (with the remaining 4 oysters reserved as extras).

150 To quantify worm infestation, oysters were submerged in a vermifuge solution of 500
151 ppm phenol, 100 ppm dichlorobenzene, and seawater for a period of 24 hours to extract
152 *Polydora websteri* from their burrows in the oyster, following methods modified from
153 Mackenzie and Shearer (1959) by Cole et al. (2020). Once extracted, *P. websteri* were hand-
154 picked from the solution, anesthetized in 7.5% magnesium chloride and then preserved in
155 ethanol to be counted later. Some *P. websteri* remained partially in their burrows in the oyster
156 after the extraction, so oysters were removed from the solution following the extraction and

157 remaining worms were counted under a microscope. Total worm abundance for each oyster was
158 calculated as the sum of the removed worms and those counted on the oyster. Because worms
159 often fragmented during extraction, only worms with heads were counted.
160 To put the blister breaking forces in context, we also measured the force required to
161 shuck the oysters. These forces were measured and recorded using a custom designed system. A
162 load cell mounted to a shucking knife measured forces applied by the blade (Fig. 2). Because we
163 wanted to measure forces under "natural" shucking conditions but also standardize our
164 measurements to reduce the error of shucking or applying force to blisters at different angles, we
165 used two different shucking methods: hand and controlled-axis. For the more natural hand
166 method, the load cell sensor was mounted near the base of a shucking knife by cutting the handle
167 just above the base, mounting the force sensor, then attaching a new handle (Fig. 2). Oysters
168 were shucked normally with the modified shucking knife while force was recorded. For the
169 controlled-axis method, oysters were held in a vice, and the knife with load sensor was
170 connected to a drill press above the vice and lowered straight down. (The drill press was not
171 turned on, so there was no rotation.) For each sampling, 6 oysters of each ploidy were shucked
172 by hand and 6 by controlled-axis. We expected that the controlled-axis method might
173 overestimate forces relative to the hand method but would yield lower variability.
174 Once oysters were shucked, tissue was discarded and photographs of the shell cavity of
175 the shucked oysters were taken (Fig. 3). ImageJ v. 1.50i software was used to determine the total
176 area of each oyster shell and the area (mm^2) of each blister, which were traced in images. A color
177 gradient with 11 steps from white to black was used to score the color of each blister (Fig. 3).
178 RGB HEX values were: 1) FFFFFF, 2) E5E5E5, 3) CCCCCC, 4) B2B2B2, 5) 999999, 6)
179 7F7F7F, 7) 666666, 8) 4C4C4C, 9) 333333, 10) 191919, and 11) 000000. Once photographed

and assigned a color, each blister was broken using the custom shucking devices described above (Fig. 2) to determine the blister breaking force. Force was measured continually while blisters were broken; peaks correspond to breaking force. Oysters that had been shucked by hand had their blisters broken using the hand-held load cell knife (Fig. 2), and oysters that had been shucked via the controlled-axis method had their blisters broken with the controlled-axis knife.

Data were analyzed using R statistical analysis software (R Core Team 2016). First a linear model was used to determine the effects of ploidy, collection site, and collection date on worm abundance. The best model was selected using the 'lm' and 'step' functions in R, which iteratively removes terms from the model based on Akaike information criterion (AIC) values. The effects of those variables plus worm abundance on blister coverage, quantified as the percent area and number of blisters, was determined in the same way. All three response variables were square-root transformed to obtain normality. When site interactions were significant, data for the three sites were analyzed separately. Similarly, shucking force was square-root transformed to obtain normality and the best linear model selected from a full model including shucking method, ploidy, site, and collection date. Data are presented as linear model coefficients with t-values indicating the significance of the slope when most of the significant variables are continuous and as ANOVA results when the variables are more categorical. ANOVA tables are provided in the Supplementary Material (S1, available online).

Because we measured breaking force on multiple blisters on each shell, breaking force data were analyzed with a linear mixed-effects model with breaking method, color, blister area, ploidy, site, and collection date as fixed effects and oyster ID as a random effect. Data were again square-root transformed to obtain normality. An initial linear mixed-effects model on breaking method, blister color, blister area, ploidy, site, and collection date was unwieldy and

had numerous interactions, so blister breaking force data were analyzed separately for hand and controlled-axis methods. Models of blister breaking force measured by both breaking methods also had significant or marginally significant ($p < 0.1$) interactions among all variables tested, so data were further split by site (NC, MI, and PAP) to examine the effects of blister color, blister area, ploidy, and collection date at each site. Interaction terms and variables that were not significant were sequentially removed from the models if their removal resulted in lower AIC values. Model outputs are provided in the Supplementary Material (S1, available online). Models were run with the lme command in the nlme toolbox (Pinheiro et al. 2019) and non-significant terms removed with the update command using R (R Core Team, 2016).

Experiment 2: Assessing blister recovery

To assess recovery of mud blisters following removal of worms, ~400 diploid and triploid oysters each were collected from Murder Point Oyster Farm in Portersville Bay, AL, (30° 22' 48.65" N 88° 18' 42.01" W) in May 2017, dipped in saturated brine solution for six minutes and allowed to air dry for 12-24 hours to kill mudblister worms. The brine dip reduced the worm abundance from 30 ± 12 to 0.2 ± 0.4 worms per oyster (mean ± st. dev., n = 24 and 16, respectively), or one worm in 3 of 16 oysters. Once treated, these oysters were redeployed at Point aux Pins oyster farm (Fig. 1) in subtidal and intertidal locations with ~100 oysters per mesh bag suspended in an alternating pattern. Every week for 9 weeks, 5 diploid and 5 triploid oysters were haphazardly selected from bags in both the intertidal and subtidal (20 oysters total). Upon collection, oysters were again transported on ice to the lab and mudblister worms were extracted using the same methods outlined in Exp. 1 above. Once worms were extracted, oysters were shucked and shells were dried on the lab bench for 48 hours. Shells were x-rayed using a

Universal HE-425 X-ray machine, set at 60 KV – 100 MA – 10 MS (the typical strength used for human wrist bones) and then photographed in full-color with a Nikon 1 J5 camera. Shells showing damage from boring sponge were excluded from analysis as the overlap of boring sponge and mudblister worm burrows were impossible to distinguish in x-ray images.

The percent of the shell covered by burrows was determined by thresholding x-ray images, and percent of the shell covered by blisters was determined by tracing blisters using ImageJ v. 1.50i. To determine what factors contributed to reinfestation of the oysters by mudblister worms, we used a linear model to assess the effects of sampling week, ploidy, location (sub- or intertidal), and total area of burrows on worm abundance. To determine whether blister coverage increased over time due to reinfestation or decreased over time from oyster recovery as well as how other variables contributed to blister recovery, we used a linear model with sampling week, ploidy, location, total area of burrows, and worm abundance as potential factors affecting blister coverage. All three variables were square-root transformed to obtain normality. The best model was selected based on lowest AIC values using the "step" function in R. Analysis was done for both the percent of shell covered by blisters and the total number of blisters.

RESULTS

Experiment 1:

Relationships among worm abundances, oyster ploidy, and mud blisters

The number of worms extracted from each oyster increased over the three collection dates ($t(208) = 13.8$, $P < 0.001$) but also showed interactions between site and collection date and

site and ploidy (see Supplementary Material, S1, available online). Splitting the data by site showed no effect of ploidy or collection date on worm abundance at Navy Cove, where abundances were very low at all three dates (Fig. 4A). At Massacre Island, worm abundances increased over the three collection dates ($t(69) = 12.18$, $P < 0.001$), and ploidy was retained in the best model but was not statistically significant ($t(69) = 1.50$, $P = 0.14$) (Table 1). Worm abundances also increased over time at Point aux Pins ($t(69) = 8.02$, $P < 0.001$) (Fig. 4A), and triploids had slightly more worms than diploids ($t(69) = 2.32$, $P = 0.023$) (Table 1). There were no pairwise differences between ploidies, although there was a slight trend toward higher worm abundances in triploids in the 3rd collection (data not shown).

The percent of the shell interior covered by blisters ranged from 0-38.3% and depended on ploidy, site, and also showed a ploidy x site interaction (step-wise linear model; see Supplementary Material S1, available online), but did not depend on collection date or number of worms extracted (Appendix Fig. A1). Site was significant only through an interaction with ploidy (2-way ANOVA; Site: $F_{2,211} = 1.82$, $P = 0.16$; interaction $F_{2,211} = 9.50$, $P < 0.001$). Triploids showed blister differences among sites, but blisters in diploids did not differ among sites (2-way ANOVA; Tukey HSD test, $\alpha = 0.05$) (Fig. 4B, Table 1). Blister coverage in triploids was highest at Point aux Pins, and blister coverage in diploids at all three sites was comparable to that in triploids from that site (Fig. 4B). Blister coverage in triploids was lowest at Navy Cove (Fig. 4B), where worm abundances were also low (Fig. 4A).

The number of blisters per oyster ranged from 0-38, and results were similar to those for blister area. Diploids had more blisters than triploids, and the number of worms extracted was positively correlated with the number of blisters, but there were also significant site x ploidy and site x worm abundance effects (see Supplementary Material S1, available online). Data were

split by site to understand the interaction terms. For Navy Cove, the best model included ploidy ($t(70) = -3.71$; $P < 0.001$) and worm abundance, which was only marginally significant ($t(70) = 1.75$, $P = 0.085$). For Massacre Island, both ploidy ($t(69) = -3.86$, $P < 0.001$) and worm abundance ($t(69) = 2.75$, $P = 0.008$) were significant. For Point aux Pins, ploidy was not included in the best model, and worm abundance was not significant ($t(70) = 1.62$, $P = 0.11$). A simplified model including only site and ploidy showed significant differences in numbers of blisters only for triploids, with no differences among sites for diploids (2-way ANOVA; Tukey HSD test, $\alpha = 0.05$) (Fig. 4C, Table 1).

Shucking and blister breaking forces

As expected, the hand method required much lower forces (median 147 N) than the controlled axis method (median 543 N) when shucking the oysters (best linear model, $F_{1,185} = 7.10$, $P < 0.001$) (horizontal lines, Fig. 5). Site and collection differences were statistically significant but much smaller than the differences between shucking methods (Appendix Fig. A2). To provide a simplified, visual qualitative comparison with blister breaking forces, we combined data from collection dates and sites and used the median and interquartile range of shucking forces for each method for comparison with blister breaking forces (Fig. 5). We expected that variability would be lower for the controlled-axis method, but shucking forces varied considerably for both methods; the interquartile range was greater for the controlled-axis method (dotted lines, Fig. 5), but normalizing the interquartile range by the median force gave fairly similar results, 0.8 for the controlled-axis and 1.2 for the hand method. Blister breaking forces also varied substantially, overlapping with the shucking forces for both methods (Fig. 5). Again, the median breaking force was higher for the controlled-axis method (218.1 N) than the

hand method (62.3 N). Variability was similar for both methods, with a higher interquartile range for the controlled axis method (182.5 N) than the hand method (40.1 N) but when normalized by the median, ranges were similar; 0.84 and 0.64, respectively.

Breaking forces for blisters from oysters collected from the eastern-most site, Navy Cove, were significantly lower for diploid than triploid oysters using the controlled-axis method ($t(24) = -2.49$, $P = 0.02$; Fig. 5A; Table 2). In contrast, using the hand method, the best model included only blister color; darker blisters broke under smaller forces ($t(186) = -3.14$, $P = 0.0019$; Fig. 5B; Table 2). From the western-most site, Point aux Pins, blister breaking forces were lower for darker blisters using both breaking methods (controlled-axis: $t(469) = -3.45$, $P < 0.001$; hand: $t(388) = -3.37$, $P < 0.001$; Fig. 5E-F, Table 2).

Models for breaking forces for blisters from oysters collected from the Massacre Island (MI) farm using both methods had significant interactions among variables, so data were further split by collection date and by ploidy (Table 2; see Supplementary Materials, S1, available online for statistics). For the controlled-axis method, both color and blister area were significant, and there was a ploidy x collection date interaction (Fig. 5C). Ploidy was not significant for any of the collection dates, but was retained in the best model with $p > 0.05$. For collection 1, blisters in diploids broke under higher forces than those in triploids, contrary to our expectation, but on subsequent dates blisters in triploids broke under higher forces (Table 2). For the hand method, there were significant interactions among color, ploidy, and date, but splitting by date showed only marginal effects or interactions among the variables (Fig. 5D; Table 2). To determine whether blister breaking forces decreased over the three collections, we also split the MI data by ploidy (Table 2). There was no effect of collection date alone for diploids, although there were some interactions (Table 2). For triploids, blister breaking forces decreased over the three

collections using the hand method but showed a marginal increase with the controlled-axis method (Table 2). In summary, for some collection dates and some methods, darker and larger blisters and those in diploids broke under smaller forces.

Experiment 2:

Reinfestation and short-term recovery

X-ray imagery of burrows showed heavy historic infestation by mud blister worms, and photos showed blisters on all shells (Fig. 6). Shells varied in their extent of burrow damage (e.g., Fig. 6A vs 6D), with some shells only showing extensive burrows in the older part of the shell (e.g., Fig. 6E, J).

Polydorid worms quickly re-infested oysters deployed subtidally, but intertidal oysters had very few worms throughout the deployment (Fig. 7A). The combined dataset had many zeros and could not be transformed to obtain normality, but worm abundance data from subtidal oysters were square-root transformed to obtain normality. Abundances in intertidal oysters were too low for further analysis. A linear model showed that worm abundances on subtidal oysters did not depend on ploidy ($t(62) = 0.95$, $P = 0.35$) or any interactions with ploidy ($P > 0.1$). A simpler model showed that worm abundance was positively correlated with sampling week ($t(66) = 2.24$ $P = 0.029$, Fig. 7A), and area of burrows ($t(66) = 3.25$, $P = 0.0018$, Fig. 7B), and the interaction was marginally significant ($t(66) = -1.96$, $P = 0.054$). Worms appeared to re-infest subtidal oysters more heavily around week 5, but then abundances were highly variable and fluctuated in subsequent weeks (Fig. 7A). That more worms were found in shells with more burrows ($p < 0.01$; $R^2 = 0.28$; Fig. 7B) is consistent with our hypothesis (H3b) that burrows would provide habitat for worms to settle.

A linear model of blister area as a function of sampling week, worm abundance, burrow area, ploidy, and sampling location (subtidal vs. intertidal) showed a significant 5-way interaction as well as numerous other interaction terms. Data were separated by location, and worm abundance was removed from the model for intertidal oysters because abundances were very low (Fig. 7). The area of blisters was positively correlated with sampling week (Fig. 8A), and area of burrows (Fig. 8B), for some but not all ploidies and locations, but did not depend on the number of worms that reinfested the oysters (Fig. 8C). The simplest model for intertidal oysters showed that blister area was higher for diploids than triploids ($t(59) = 3.33$, $P = 0.0015$), showed a positive relationship with area of burrows ($t(59) = 4.57$, $P < 0.001$), and a significant ploidy x burrow area interaction ($t(59) = -2.85$, $P = 0.0061$), but showed no effect of sampling week (Fig. 8A). Data were separated by ploidy to understand the interaction term, and blisters depended on burrows only for triploid oysters ($t(33) = 5.26$, $P < 0.001$, $r^2 = 0.44$) but not for diploids ($t(26) = 1.21$, $P = 0.23$, $r^2 = 0.02$) (Fig. 8B). For subtidal oysters, the best model showed a positive correlation with area of burrows ($t(67) = 4.33$, $P < 0.001$) (Fig. 8B) and week ($t(67) = 4.78$, $P < 0.001$) (Fig. 8A); neither ploidy nor worm abundances (Fig. 8C) nor any interactions significantly affected blister coverage in subtidal oysters.

DISCUSSION

Our data showed some support for all four hypotheses, although in some cases support was weaker than we expected. Worm abundances did exceed blister numbers and the two were poorly correlated, consistent with not all worms creating a blister (H1). Triploids had less blister damage than diploids (presumably due to faster growth rates and blister recovery) and in some cases blisters broke under higher forces than for diploids (H2). These differences were not as

364 consistent as we expected, likely due to high worm reinfestation during the summer when these
365 experiments were conducted. Worm reinfestation was greater in subtidal than intertidal oysters
366 as well as in previously infested oysters, resulting in greater blister damage (H3). We measured
367 blister breaking forces as a proxy for recovery, predicting that darker and larger blisters would
368 break under smaller forces (H4). Although we did find significant effects of blister color and area
369 consistent with our hypothesis, blister breaking forces were low (comparable to or lower than
370 shucking forces) for most of the experiment. The experiment was conducted in the summer when
371 worm infestation rates were increasing, potentially contributing to low blister breaking forces.
372
373 ***Worm abundances are only weakly correlated with blister coverage***
374 We found no relationship between blister damage and worm abundance, as assessed by
375 the number of worms at the time sampled (Fig. A1), although there was a weak relationship
376 between blister damage and the historical record of worm infestation shown through X-ray
377 images of burrows (Fig. 7B). Moreover, the number of worms per oyster exceeded the number of
378 blisters by over an order of magnitude (Fig. 4A, C), consistent with our hypothesis (H1) that not
379 all worms create blisters. This decoupling of worm abundance and blister coverage suggests that
380 most worms bore into oysters by settling on crevices on the outer surface of the shell, consistent
381 with descriptions by Zottoli and Carriker (1974) and Hopkins (1958). X-ray images show
382 burrows oriented in all different directions (Fig. 6), consistent with only a small number of
383 burrows penetrating far enough through the shell to form a blister. Diez et al. (2013) found 4-5
384 *Polydora rickettsi* in each mudblister in scallops, and it is plausible that multiple *P. websteri*
385 contribute to each mud blister in these oysters as well. Submerging oysters in water before
386 extracting worms reveals lines of palps extending from circular burrow openings (~0.5 mm

387 diam.) that run along crevices in the shell (Morse *et al.*, 2015) – while these burrows are too
388 difficult to see to accurately count, it does appear that there are many burrow openings within the
389 area of an average-sized mud blister (K.D., pers. obs.).
390 Although we expected that worm abundance would cause greater blister coverage, in fact
391 stronger relationships between worm abundance and burrows (Fig. 7B) and between burrows and
392 blisters (Fig. 8B) suggest that more blisters may reflect prior infestation and therefore more
393 burrow space for new worms to recruit. Thus, it seems more likely that the weak relationship
394 between worm abundance and blisters was driven by blisters from previous infestation causing
395 higher worm abundances rather than by worms creating new blisters. The presence of burrows
396 facilitating settlement of new worms is consistent our hypothesis (H3b) and with previous
397 studies (Simon et al., 2006, Cole et al., 2020).
398
399 ***Short-term shell repair: effects of ploidy and worm reinfestation on blister damage***
400 Fewer blisters in triploid oysters than in diploids (Fig. 4B, C) supports our hypothesis
401 (H2) that faster-growing triploids would secrete new shell layers to cover blisters more quickly
402 than diploids. Higher growth rates of triploid oysters do not, however, result in lower worm
403 infestation rates, consistent with our previous study (Cole et al., 2020). Since worm infestation
404 does not differ with ploidy, it follows that blister formation does not differ with ploidy and that
405 these differences reflect faster recovery in triploids. The site with the fewest worms, Navy Cove,
406 had the most notable differences in blister coverage and number of blisters between diploids and
407 triploids (Fig. 4B, C) as well as higher blister breaking forces for triploids (Fig. 5A); new blisters
408 caused by the abundant worms at the other two sites in both diploids and triploids likely
409 decreased the differences resulting from faster recovery in triploids. While blister breaking

forces were highly variable, we did find some instances in which blisters in triploids broke under larger forces than those in diploids (Table 2), consistent with greater recovery in triploids. This is consistent with observations by oyster farmers that they find less blister damage by mud blister worms in triploid than in diploid oysters.

Following treatment of oysters, worms re-infested those deployed subtidally within a few weeks but either did not reinfest those deployed intertidally or, more likely, did not survive the periodic air exposure (Fig. 7), consistent with previous studies (Handley and Bergquist, 1997; Gamble 2016). Increasing blister damage in subtidally-deployed oysters over the duration of our redeployment (Fig. 8A) indicated that worms that reinfested the oysters were creating new blisters in a relatively short amount of time. We were surprised, however, to find no clear blister recovery in the oysters deployed intertidally that were not reinfested (Fig. 8A). This suggests that blister recovery happens very slowly, although oysters deployed in the high intertidal have been shown to have lower growth rates than those grown subtidally (Bartol et al. 1999); shell repair may happen more quickly under conditions more conducive to oyster growth. Oysters, as well as oyster-growers, may face a trade-off, with lower infestation but also lower recovery in the intertidal compared to subtidal.

Within subtidal oysters, more worms were found in oysters that had more burrows, consistent with our hypothesis (H3b) that worms would take advantage of existing burrows when settling and would preferentially settle or have higher survival on oysters that had been previously infested (cf., Cole et al., 2020). Shells that had more burrows also had more blisters (Fig. 8B), although since this was true for triploids deployed intertidally that were not re-infested and we did not see blister recovery for the intertidal oysters (Fig. 8A), this correlation likely reflects the pre-treatment infestation. It is important to note that our comparisons were among

oysters deployed under the same conditions rather than within individual oysters, which is not possible because oysters need to be shucked to see the blisters. Variability in both worm infestation and blister coverage was very high both in the field-collected oysters (Fig. 4) and in the treated and re-deployed oysters (Fig. 7, 8). Considerable variability in burrow damage among shells is apparent in the X-ray images: although some shells had burrows primarily in the older region (e.g., Fig. 6E), other shells showed burrow damage throughout the shell (Fig. 6H). Positive feedbacks in which previously infested oysters become infested preferentially could increase variability in worm abundance and blister damage within oysters at one site. However, the effects of blister damage can be exacerbated by other stressors, e.g., the endoparasite *Haplosporodium nelsoni* (Wargo and Ford, 1993); we removed several shells from our X-ray analysis due to damage by boring sponges but did not explicitly look for other parasites or biofoulers in this study.

Blister breaking forces as indicators of recovery

We predicted that smaller, lighter colored blisters would have "recovered" in strength and therefore would require larger forces break than applied when shucking the oysters. We did find some significant effects of color consistent with our hypothesis (Table 2), however, most of the measured blister breaking forces were lower than or within the range of shucking forces measured (Fig. 5). We expected some breaking forces to be lower than shucking forces, as breaking blisters while shucking oysters is a known problem for the half-shell market, but were surprised that blisters of all colors and sizes broke under smaller forces than required to shuck the oysters. Thus, visually distinguishing between blisters that would break during shucking and those that would not break does not seem feasible. The thickness of the nacreous layer overlying

456 the blister is likely the most important factor affecting blister breaking force. We had expected
457 that darker blisters would have thinner nacreous layers, as suggested by Handley and Bergquist
458 in their study examining blisters in *Crassostrea gigas* in northern New Zealand (1997). Whereas
459 Handley and Bergquist (1997) described a bimodal distribution of blister colors, blisters in our
460 study spanned the range of colors (Fig. 3, 5, 6). One possible explanation is that whereas larval
461 worms were only found during summer in New Zealand (Handley and Bergquist, 1997), larval
462 *P. websteri* are found year-round in coastal Alabama (Cole et al. 2020) and Louisiana (Hopkins,
463 1958). These differences in blisters could reflect annual versus continuous larval settlement on
464 oysters and formation of new blisters. Infestation peaks in the summer in coastal Alabama (Cole
465 et al. 2020) and many other locations (Blake 1969, Handley and Bergquist 1997), thus any
466 recovery that may have occurred over the winter and spring when infestation was lower may
467 have been masked by the new infestation causing new blister damage during the time of our
468 study (cf. Fig. 4A, 8A). Reinfestation of existing burrows would likely weaken blister strength,
469 and if multiple worms contribute to one blister, this could increase variability in breaking
470 strength or decouple color from breaking strength. It is also possible that the amount of sediment
471 that the worm brings into the burrow may vary, affecting blister color. We did not attempt to
472 measure the thickness of the shell overlying the blister after breaking it, but our data suggest that
473 this would be interesting to attempt in future experiments. It is possible that measuring blister
474 shell thickness rather than using color as a proxy would better predict blister breaking forces.
475 Our method of measuring blister breaking forces was simple, low-cost, and has the
476 potential to be useful in further studies of blister recovery. We expected that variability would be
477 greater with the hand breaking method because of variability in hand positioning when blisters
478 were broken. This was not the case, perhaps because high variability in blister strength (Fig. 5)

exceeded any variability from hand positioning. Thus, the method of breaking blisters with the force sensor embedded into the shucking knife seems to be preferable as it is more realistic, but not more variable, than the controlled-axis method.

Implications and future work

The aim of this study was to explore the dynamics of mud blister formation and recovery, but the study was conducted in the summer as worm infestation was increasing (Fig. 4A), thus our results reveal more about the formation process than recovery. Our findings that triploid oysters had fewer blisters (despite no differences in vulnerability to infestation) and in some cases higher blister breaking forces than diploids support observations by oyster farmers that triploids had less blister damage than diploids and indicates that the investment in faster-growing triploids may be beneficial in reducing blister damage. The decoupling of worm abundances and blister damage indicate that worm abundances may not be the best indicator of mudblister damage, and that damage may last much longer than the worms themselves. Recruitment of worms to previously infested shell may increase variability in worm abundances and blister damage among oysters within a site and suggest that treatments of oysters early in their deployment may be particularly important in reducing cumulative damage from mudblister worms.

We found little indication of shell recovery over the short duration of these experiments, based on increasing shell damage over time for treated oysters (Fig. 8A) and variable but low blister breaking forces (Fig. 5). This was likely driven by increasing worm infestation over the duration of our experiments, masking any recovery process. Our novel method of measuring blister breaking forces is simple and low-cost, and we hope it will be applied to study blister

strength in different systems. Future studies examining temporal patterns in worm abundance, blister coverage, and blister strength over longer time periods, especially during times of low worm abundance, would be useful in better assessing blister recovery. Experiments conducted in cooler waters in which mud blister worms show clearer seasonal patterns (e.g., Blake 1969, Handley and Bergquist 1997) may be more successful in decoupling recovery from reinfestation and blister formation.

ACKNOWLEDGEMENTS

We thank Erin Kiskaddon for her helpful edits on the manuscript and for making Figure 2. We also thank anonymous reviewers for constructive feedback on the manuscript. We also thank Urgent Care by the Bay (Daphne, Alabama) for the generous use of their equipment and assistance to complete this project. We also thank Viktoria Bogantes for confirming our species identification and providing the COI sequence for *P. websteri* from Dauphin Island. This publication was supported by the U.S. Department of Commerce's National Oceanic and Atmospheric Administration under NOAA Award NA18OAR4170080 and the Mississippi-Alabama Sea Grant Consortium and by NSF REU award #1838618. The views expressed herein do not necessarily reflect the views of any of these organizations.

REFERENCES

Bailey-Brock, J. H. and A. Ringwood. **1982**. Methods for control of the mud blister worm, *Polydora websteri*, in Hawaiian oyster culture. *Sea Grant Quarterly* **4**: 1–6.

Bartol, I., Mann, R., Luckenbach, M. 1999. Growth and mortality of oysters (*Crassostrea virginica*) on constructed intertidal reefs: effects of tidal height and substrate level. *Journal of Experimental Marine Biology and Ecology* 237(2), 157-184.

Bergman, K. M., R. W. Elner and M. J. Risk. 1982. The influence of *Polydora websteri* borings on the strength of the shell of the sea scallop, *Placopecten magellanicus*. *Can J Zool* 60: 2551–2556.

Blake J, Evans J. 1973. *Polydora* and other related Polychaeta Spionidae as borers in mollusk shells and other calcareous substrates. *Veliger* 15:235-249.

Brown, S.W. 2012. Salinity tolerance of the oyster mudworm *Polydora websteri.* University of Maine MS thesis, 39 pp.

Cole, S., Dorgan, K., Walton, W., Dzwonkowski, B., Coogan, J. 2020. Seasonal and spatial patterns of mudblister worm Polydora websteri infestation of farmed oysters in the northern Gulf of Mexico. *Aquaculture Environment Interactions* **12**, 297-314.

Diez, M. E., J. M. Orensanz, F. Márquez and F. Cremonte. 2013. Shell damage in the Tehuelche scallop *Aequipecten tehuelchus* caused by *Polydora rickettsi* (Polychaeta: Spionidae) infestation. *J Invertebr Pathol* 114: 107–113.

Gamble, C. R. 2016. An evaluation of the floating cage system for eastern oyster (Crassostrea virginica): Aquaculture production in the north-central Gulf of Mexico. Auburn University, AL, MS thesis, 121 pp.

Haigler, S. A. 1969. Boring Mechanism of *Polydora websteri* Inhabiting *Crassostrea virginica*. *Integrative and Comparative Biology* **9**: 821–828.

Handley, S. J. and P. R. Bergquist. **1997**. Spionid polychaete infestations of intertidal pacific oysters Crassostrea gigas (Thunberg), Mahurangi Harbour, northern New Zealand. *Aquaculture* **153**: 191–205.

Hopkins, S. H. 1958. The planktonic larvae of *Polydora websteri* Hartman (Annelida, Polychaeta) and their settling on oysters. *Bull. Mar. Sci.* **8**: 268–277.

Hopkins, T.S., J. F. Valentine, and L. B. Lutz. 1989. An illustrated guide with key to selected benthic invertebrate fauna of the northern Gulf of Mexico. Mississippi-Alabama Sea Grant Consortium, MASGP-87-010, 163pp.

Lunz, G. R. 1941. *Polydora*, A pest in South Carolina oysters. *J. Elisha Mitchell Sci. Soc.* **57**: 273–283.

Martinelli J, Lopes H, Hauser L, Jimenez-Hidalgo I, King TL, Padilla-Gamino J, Rawson P, Spencer L, Williams J, Wood C. 2019. Confirmation of the shell-boring oyster parasite *Polydora websteri* (Polychaeta: Spionidae) in Washington State, USA. Scientific Reports 10(1), 3961

Morse, D. L., P. D. Rawson and J. N. Kraeuter. **2015**. Mud Blister Worms and Oyster Aquaculture. *Maine Sea Grant Publications*, Maine Sea Grant **46**.

Pinheiro J, Bates D, DebRoy S, Sarkar D, R Core Team. 2019. *nlme: Linear and Nonlinear Mixed Effects Models*. R package version 3.1-131. Available: https://CRAN.R-project.org/package=nlme [2017, Feb 7].

R Core Team. **2016**. R: A language and environment for statistical computing. R Foundation for

565 Statistical Computing, Vienna, Austria. Available: https://www.R-project.org/. Accessed
566 [2016, June 12].

567 **Radashevsky, V. 1999.** Description of the proposed lectotype for *Polydora websteri* Hartman in
568 Loosanoff & Engle, 1943 (Polychaeta: Spionidae) *Ophelia* 51(2), 107-113.

569 **Rice, L. N., Lindsay, S., and P. Rawson. 2018.** Genetic homogeneity among geographically
570 distant populations of the blister worm Polydora websteri. *Aquacult. Env. Interac.*, **10**: 437–
571 446.

572 **Simon, C. A., Ludford, A., and S. Wynne. 2006.** Spionid polychaetes infesting cultured
573 abalone *Haliotis midae* in South Africa. *Afr. J. Mar. Sci.*, **28(1)**: 167–171.

574 **Simon, C. A., and W. Sato-Okoshi. 2015.** Polydorid polychaetes on farmed molluscs:
575 distribution, spread and factors contributing to their success. *Aquacult. Env. Interac.*, **7(2)**:
576 147–166.

577 **Stone, B. W., N. H. Hadley and P. R. Kingsley-Smith**. **2013**. Evaluating the Potential Growth
578 Advantage of Triploid Eastern Oysters (*Crassostrea virginica*) in South Carolina Relative to
579 Commercially Cultured Diploid Native Stocks. *J. Shellfish Res.* **32**: 647–655.

580 **Walton, W. C., F. S. Rikard, G. I. Chaplin, J. E. Davis, C. R. Arias and J. E. Supan**. **2013**.
581 Effects of ploidy and gear on the performance of cultured oysters, *Crassostrea virginica*:
582 Survival, growth, shape, condition index and Vibrio abundances. *Aquaculture* **414-415**: 260–
583 266.

584 **Wargo, R. N. and S. E. Ford**. **1993**. The effect of shell infestation by *Polydora* sp. and infection
585 by *Haplosporidium nelsoni* (MSX) on the tissue condition of oysters, *Crassostrea virginica*.
586 *Estuaries* **16**: 229.

587 **Watson, D. I., S. E. Shumway and R. B. Whitlatch**. **2009**. Biofouling and the shellfish
588 industry. In: *Shellfish Safety and Quality*, pp. 317–337. Woodhead Publishing, Cambridge,
589 UK.

590 **Zottoli, R. A. and M. R. Carriker**. **1974**. Burrow morphology, tube formation, and
591 microarchitecture of shell dissolution by the spionid polychaete *Polydora websteri*. *Mar.*
592 *Biol.* **27**: 307–316.

593

594 **FIGURE CAPTIONS**

595 **Figure 1:** Map of oyster farms along the Alabama coast, including Point aux Pins (30°22'58.5"N

596 88°18'46.2"W), Massacre Island (30°15'13.5"N 88°10'08.7"W), and Navy Cove (30°13'59.0"N

597 87°58'45.2"W).

598

599 **Figure 2:** Schematic of hand method of measuring forces during shucking and breaking blisters
600 with wiring diagram for the force sensor. Force measurements were made utilizing a 250-lb
601 Futek LCM300 inline load cell (Futek Advanced Sensor Technology, Inc., Irvine, CA) connected
602 to an Arduino UNO board with an INA125P amplifier (Texas Instruments Inc., Dallas, TX) and
603 custom Arduino and Processing (Processing Foundation) software to record force measurements.
604 For the controlled-axis method, the handle is replaced with a mount to the drill press.

605

606 **Figure 3:** Color scale used to score blisters with examples of blisters (some outlined with dotted
607 lines) with their color score. Scale bar = 1 cm.

608

609 **Figure 4**: (A) The number of worms per oyster differed among sites and increased over the three
610 collection dates at Massacre Island (MI) and Point aux Pins (PAP), remaining low at Navy Cove
611 (NC). (B) The percent of the shell covered with blisters varied among sites for triploids but did
612 not differ among diploid oysters. (C) The number of blisters per oyster showed similar patterns.
613 Letters indicate significant differences (Tukey HSD test, $\alpha = 0.05$, 2-way ANOVA).

614

615 **Figure 5.** Blister breaking force plotted as a function of blister color and oysters from Navy
616 Cove (A, B), Massacre Island (C, D), and Point aux Pins (E, F) for the controlled axis breaking
617 method (A, C, E) and the hand breaking method (B, D, F). Solid and dotted horizontal lines
618 indicate the median and quartiles of shucking force for each method. Blisters in diploid oysters
619 are shown as open circles slight left of the vertical line for each color, in triploid oysters as dark

triangles slightly right of the vertical line. Statistical analyses were done on square-root transformed data, but graphs show non-transformed data.

Figure 6: Left (A-E) and right (F-J) valves of oysters, with photo images on the left and corresponding X-ray images from the same shell on the right. Images of shells are rotated and scaled to align, scale bar = 1 cm.

Figure 7: Worms per oyster plotted as a function of (A) sampling week, and (B) percent of shell covered with burrows. Data from oysters deployed subtidally are shown in gray, for oysters deployed intertidally in black. A significant positive correlation between worm abundance and the percent of the shell covered with burrows for subtidal oysters is plotted as a gray line ($p < 0.01$). Statistics were done on square-root transformed data.

Figure 8: Percent of shell area covered with blisters as a function of (A) sampling week, (B) percent of shell area covered with burrows, and (C) worm abundance. Data were separated by ploidy and deployment location, and significant relationships ($p < 0.05$) are plotted as solid (triploid) or dashed (diploid), gray (subtidal) or black (intertidal) lines. Note that the y-axis is not linear because data were square-root transformed.

Appendix Figure A1: Blister cover did not depend on the number of worms extracted for each oyster. Oysters from Massacre Island (MI) are plotted as circles, from Point aux Pins (PAP) plotted as squares, diploid oysters with white fill, triploid oysters with gray fill. Oysters from Navy Cove (NC) had very low worm abundances, so were not included in the plot.

643

644 **Appendix Figure A2**: Square-root transformed shucking force plotted as a function of site and
645 collection (shading) date for (A) hand method, and (B) controlled-axis method of shucking. Site,
646 collection date, and a shucking method x collection date interaction were all significant in the
647 model to explain shucking force, so data were split by shucking method and analyzed separately.
648 For the hand method, shucking forces were lower for oysters from Point aux Pins than for those
649 from Navy Cove (Tukey HSD test, $\alpha = 0.05$). For the controlled-axis method, shucking forces
650 were slightly lower during collection 1 than the later collection dates, and were slightly higher at
651 Navy Cove than at the other two sites (Tukey HSD test, $\alpha = 0.05$).

652

653 **Supplemental S1, available online**: Linear model and linear mixed-effect model result tables.

Table 1: Model results showing the significance of independent variables: collection date, ploidy, site, and worm abundance on the dependent variables: worm abundance, percent of the shell covered by blisters, and number of blisters. All three showed interactions with site and were split by site for further analysis. * indicates significant effect, i is a significant interaction, m is a marginal effect (term included in best model but $p > 0.05$), - is no effect. Terms not included in the model are left blank.

		Date	Ploidy	Site	# worms
Worm abundance		i	i	i	
	MI	*(+)	m ($t \geq d$)		
	NC	-	-		
	PAP	*(+)	* ($t > d$)		
% blisters		-	i	i	-
	MI	-	* ($d > t$)		-
	NC	-	* ($d > t$)		-
	PAP	-	-		-
# blisters		-	i	i	i
	MI	-	* ($d > t$)		* (+)
	NC	-	* ($d > t$)		m (+)
	PAP	-	-		m (+)

Table 2: Blister breaking force model results, showing independent variables tested for their effect on blister breaking force. Data were split by blister breaking method (columns) and site. For MI, data were further split by collection date and ploidy because of significant interactions. * indicates significant effect, m is marginally significant (retained in best model but $p > 0.05$). With the exception of ploidy for MI Coll 1 Controlled-axis (where d > t indicates that forces in diploids were larger than in triploids), all effects were consistent with hypotheses. i is a significant interaction, - is no effect. Terms not included in the model are left blank.

Site	Split by	Controlled axis method				Hand method			
		color	ploidy	area	date	color	ploidy	area	date
NC		-	*	-	-	*	-	-	-
MI		*	i	*	*i	*i	*i	-	i
MI	Coll 1	-	m (d>t)	*		m	m	-	
MI	Coll 2	*i	m	*i		i	-	i	
MI	Coll 3	*	m	*		-	m	-	
MI	Dip	i		*	i	i*		-	i
MI	Trip	m		*	m(+)	i		i	*(-)
PAP		*	-	-	-	*	-	-	-

Figure 1

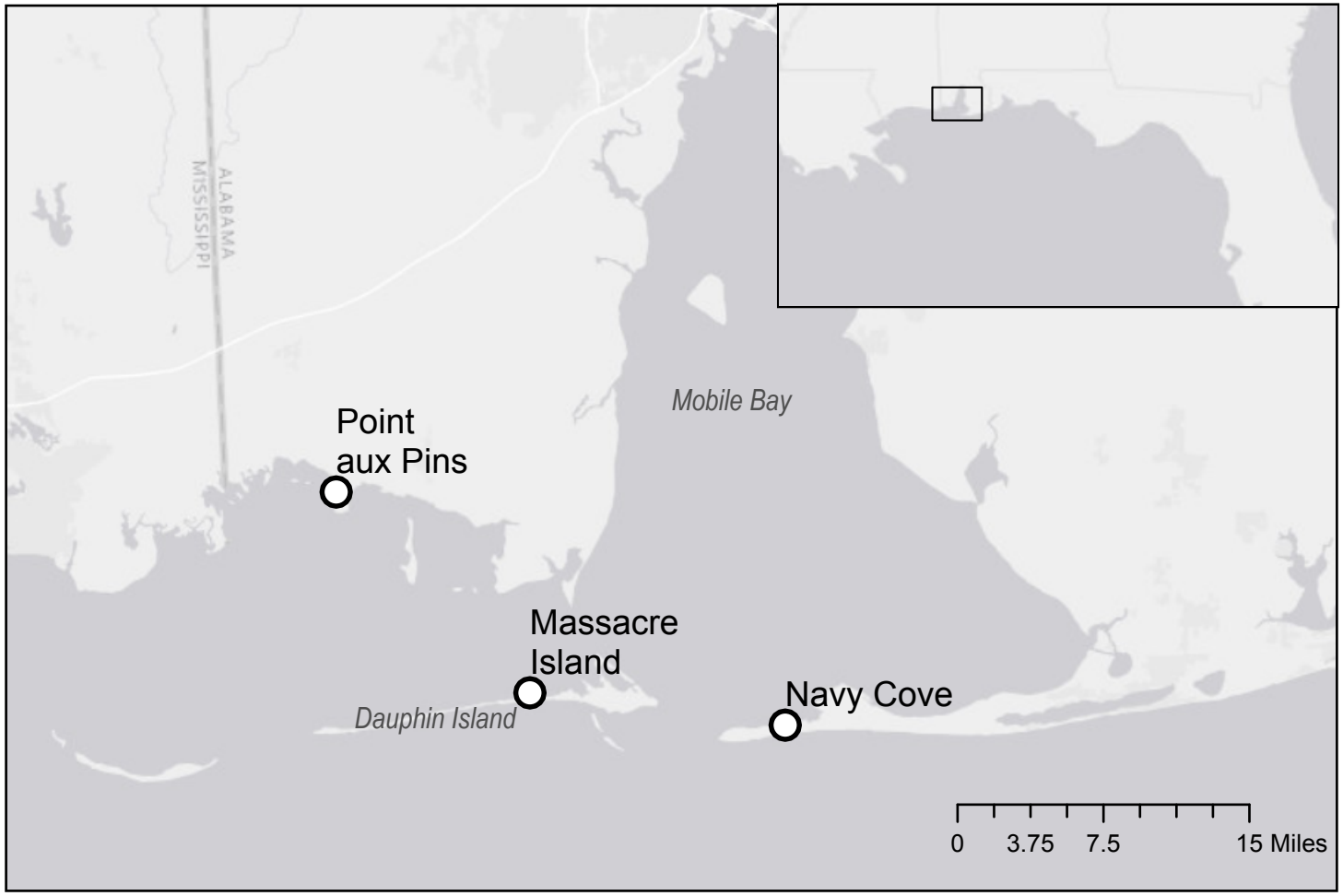
ALABAMA
MISSISSIPPI
Mobile Bay
Point
aux Pins
Massacre
Island
Dauphin Island
Navy Cove
0
3.75
7.5
15 Miles

Figure 2

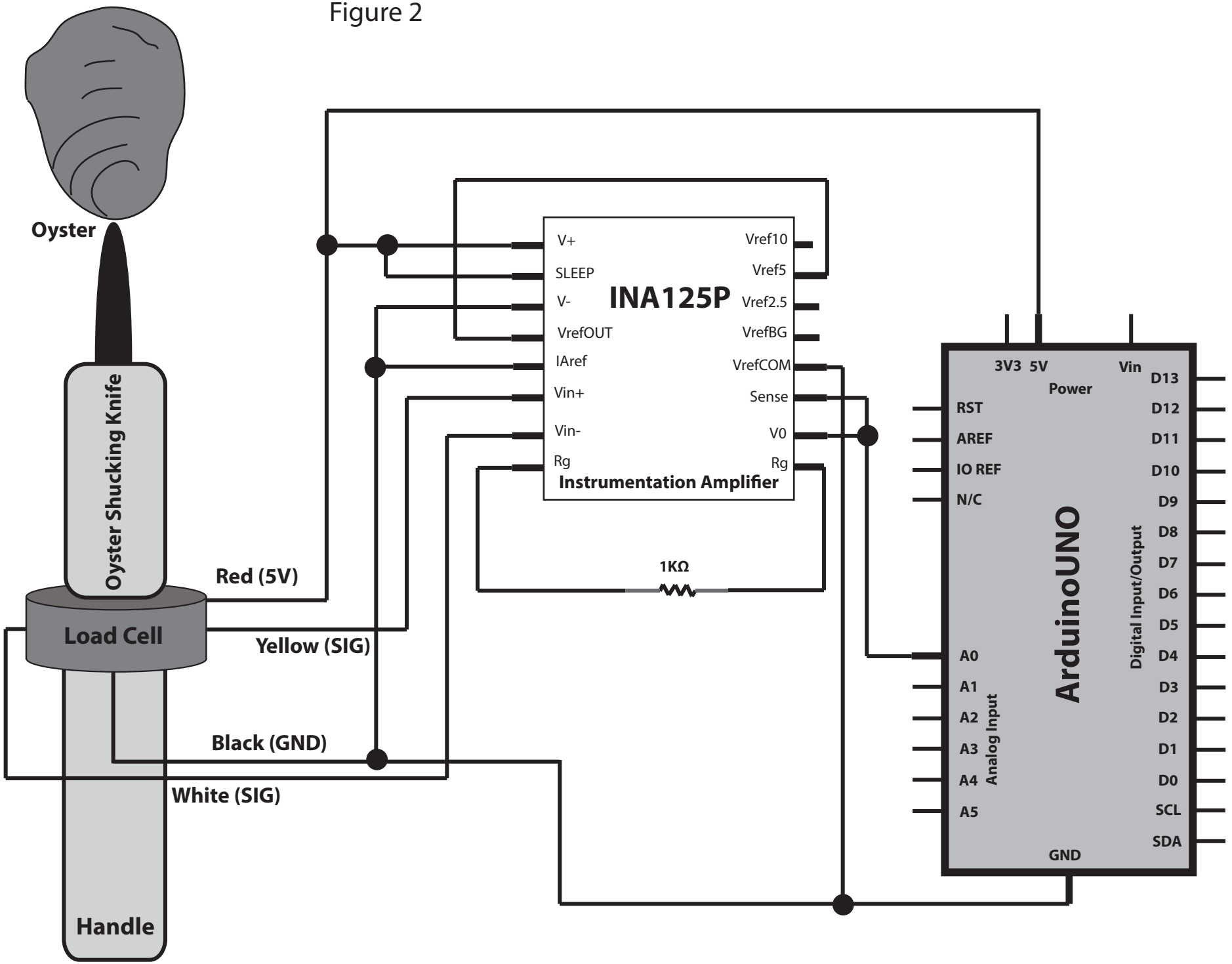
Oyster
Oyster Shucking Knife
Load Cell
Handle
Red (5V)
Yellow (SIG)
Black (GND)
White (SIG)
INA125P
V+
SLEEP
V-
VrefOUT
IAref
Vin+
Vin-
Rg
Vref10
Vref5
Vref2.5
VrefBG
VrefCOM
Sense
V0
Rg
Instrumentation Amplifier
1KΩ
ArduinoUNO
3V3
5V
Power
Vin
RST
AREF
IO REF
N/C
A0
A1
A2
A3
A4
A5
Analog Input
GND
D13
D12
D11
D10
D9
D8
D7
D6
D5
D4
D3
D2
D1
D0
SCL
SDA
Digital Input/Output

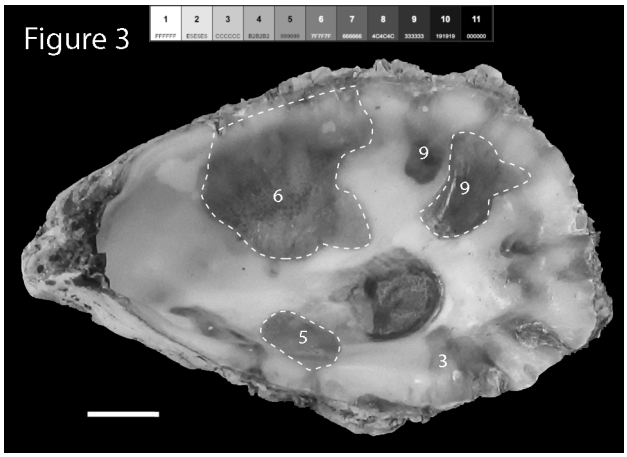
Figure 3
1
2
3
4
5
6
7
8
9
10
11
6
9
9
5
3

Figure 4

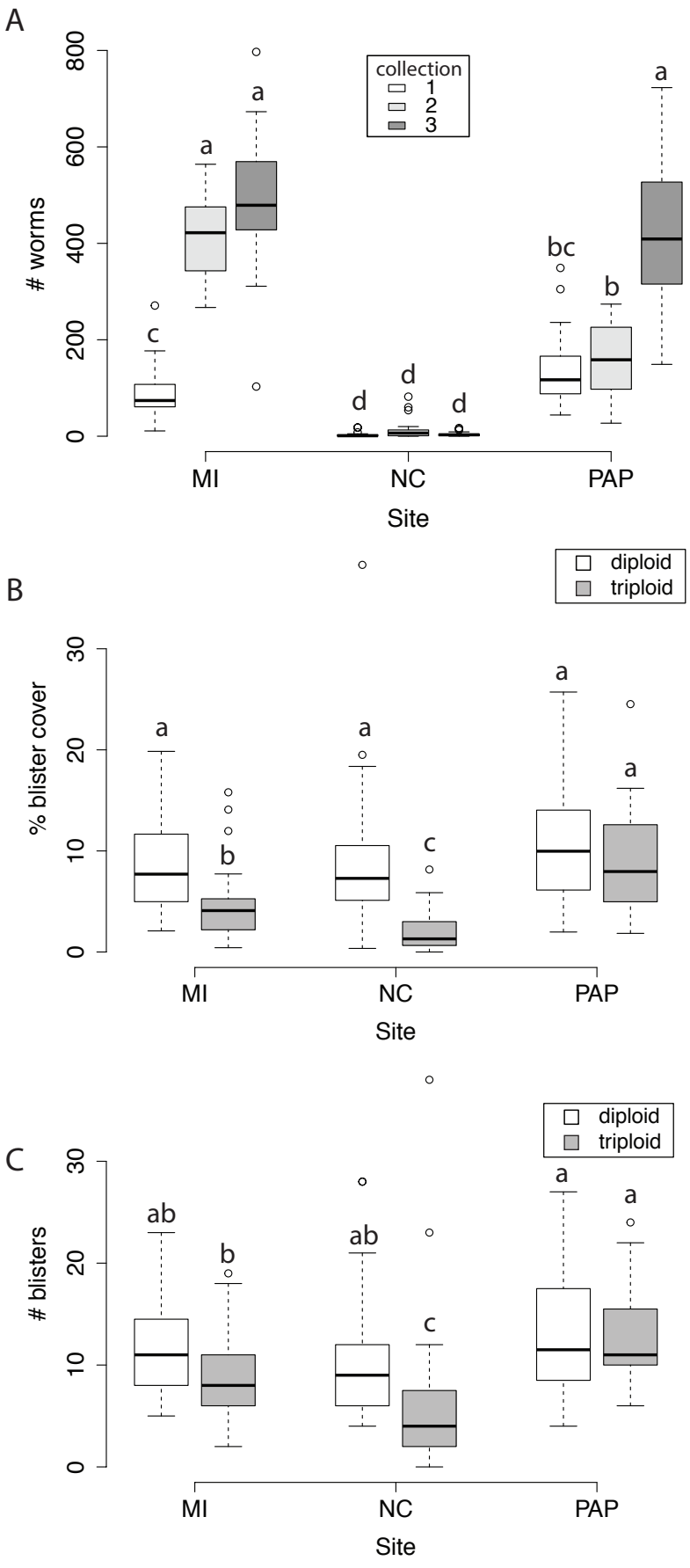
A
worms
0
200
400
600
800
collection
1
2
3
c
a
a
d
d
d
bc
b
a
MI
NC
PAP
Site
B
% blister cover
0
10
20
30
diploid
triploid
a
b
a
c
a
a
MI
NC
PAP
Site
C
blisters
0
10
20
30
diploid
triploid
ab
b
ab
c
a
a
MI
NC
PAP
Site

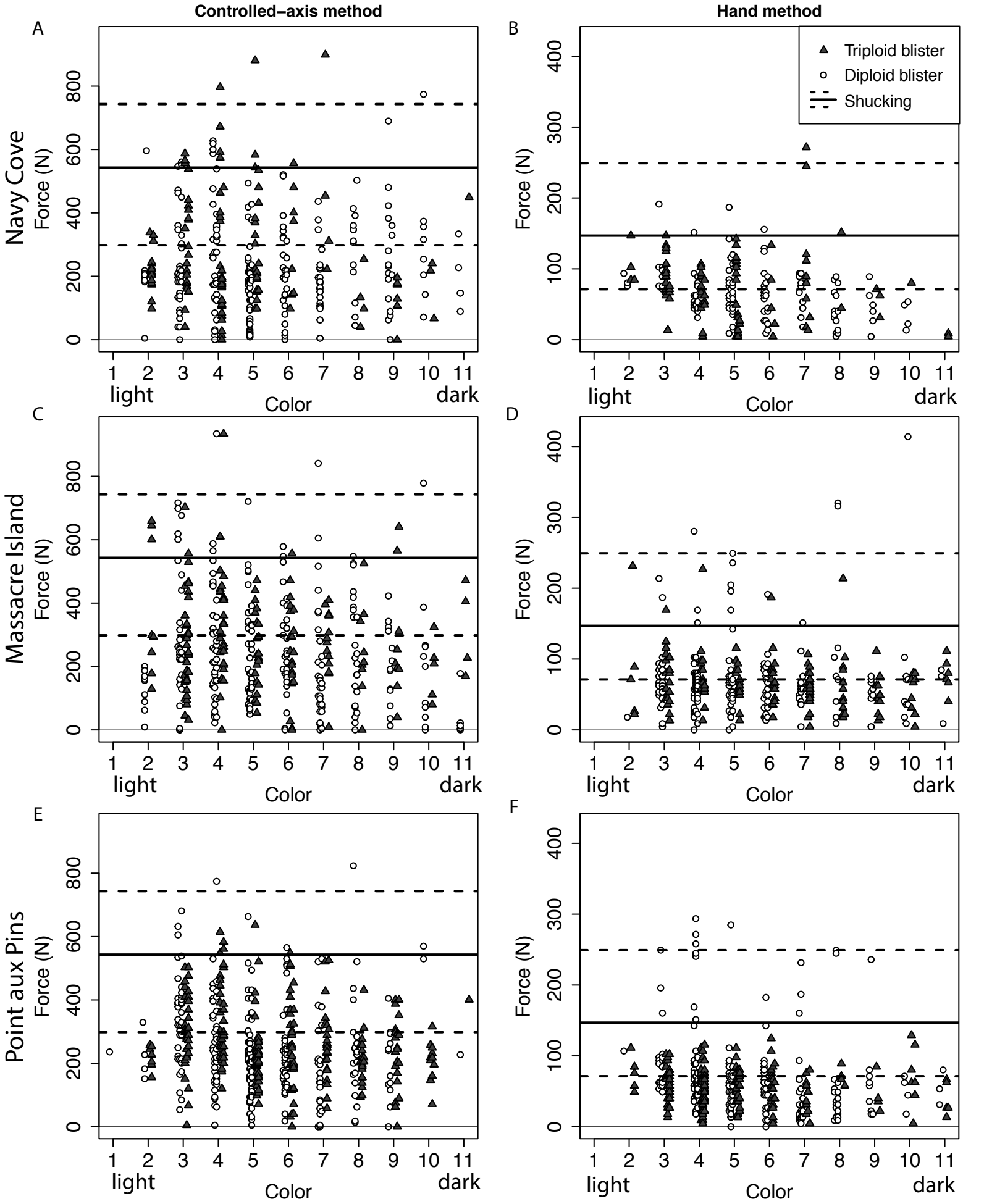
Controlled−axis method
Hand method
A
B
C
D
E
F
Navy Cove
Massacre Island
Point aux Pins
Force (N)
Color
light
dark
Triploid blister
Diploid blister
Shucking

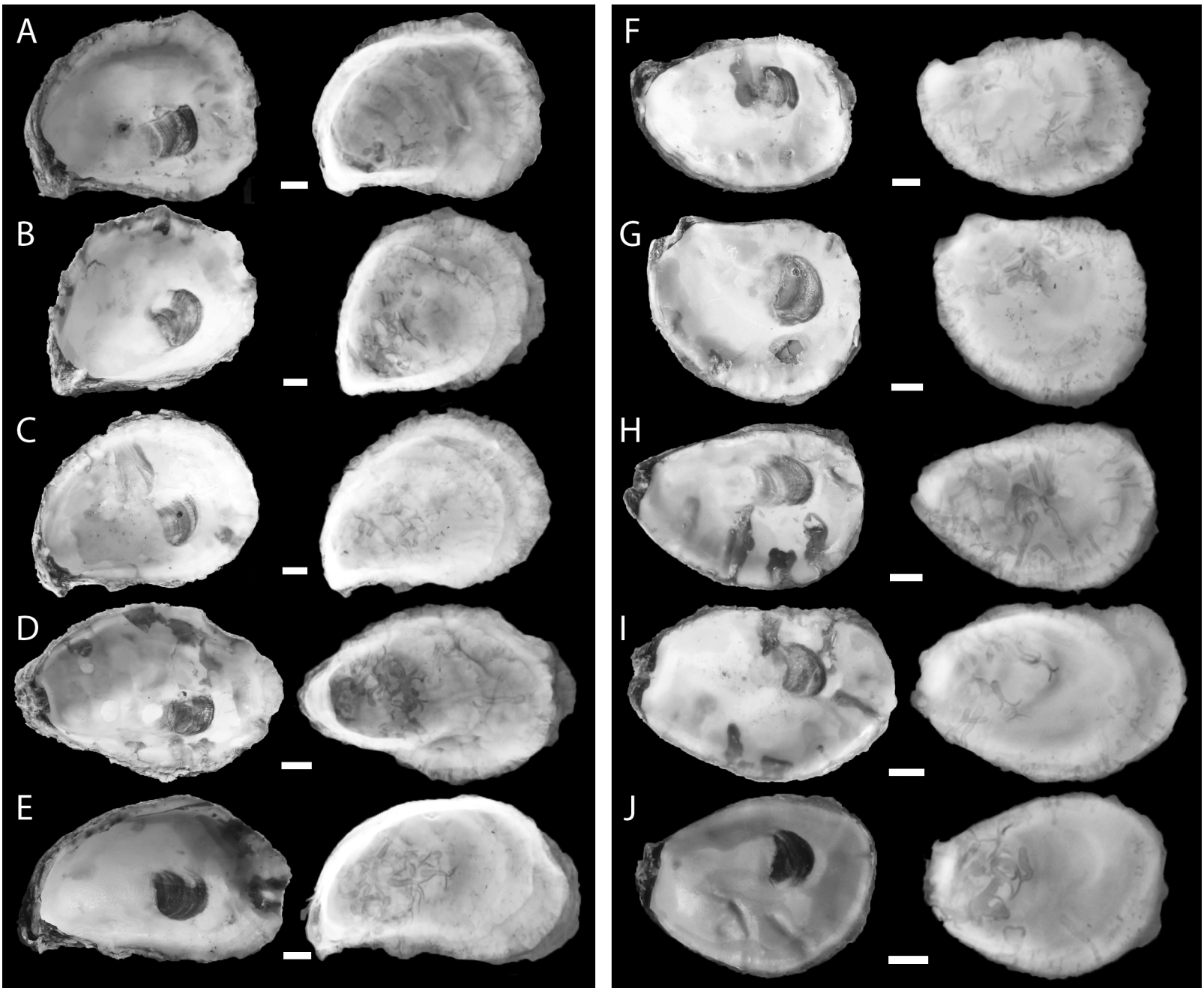
A
B
C
D
E
F
G
H
I
J

Figure 7

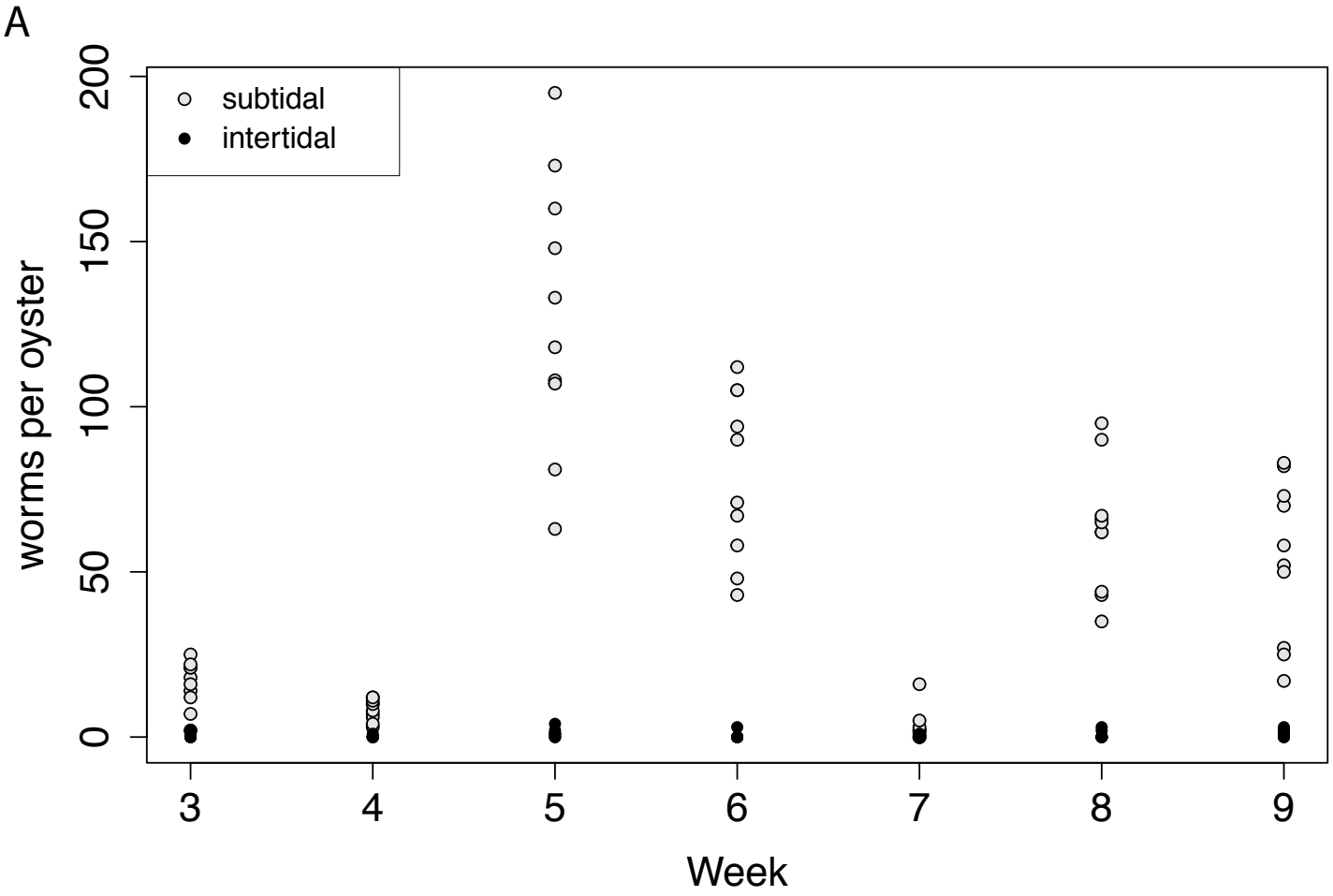
A
subtidal
intertidal
worms per oyster
0
50
100
150
200
3
4
5
6
7
8
9
Week

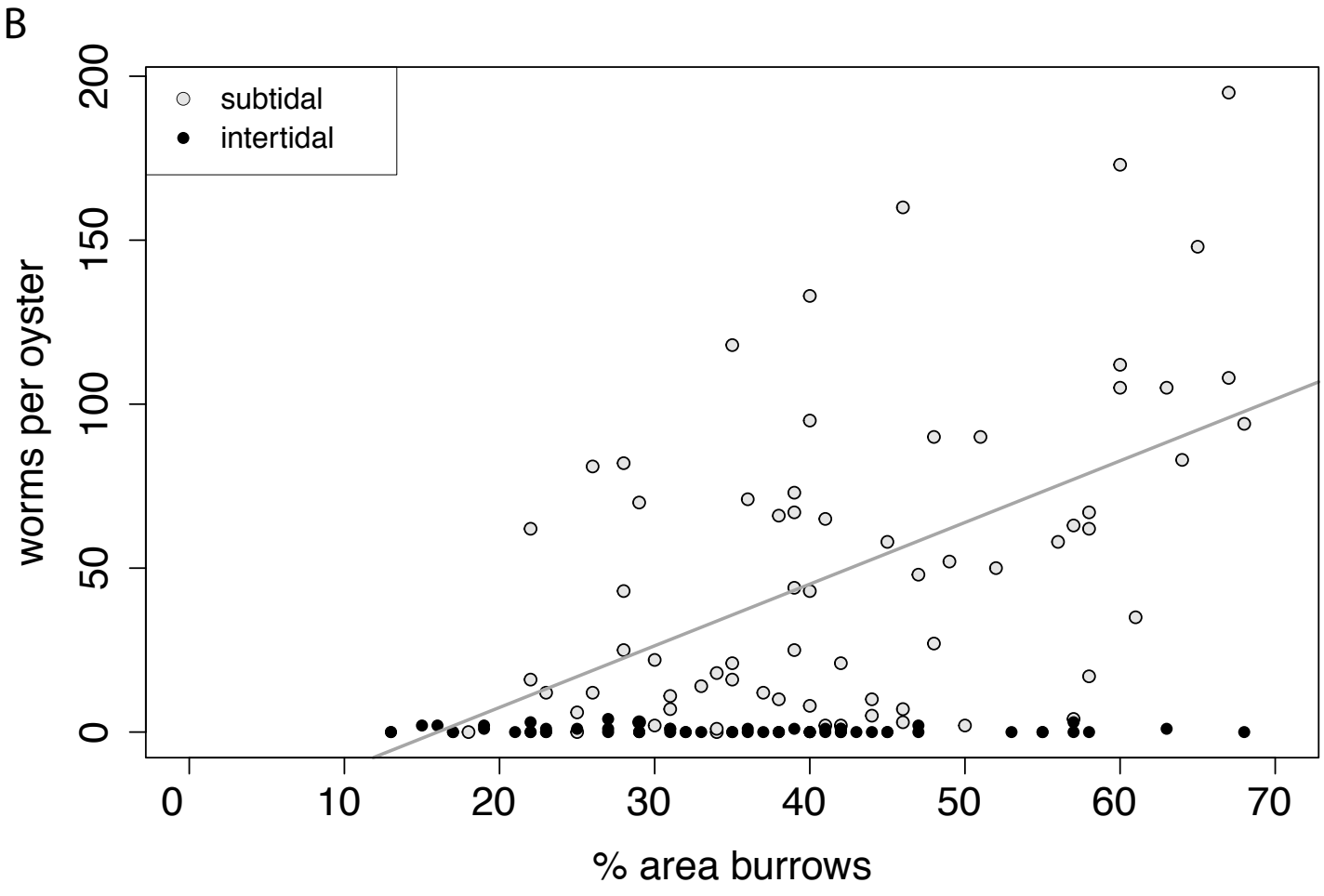
B
subtidal
intertidal
worms per oyster
0
50
100
150
200
0
10
20
30
40
50
60
70
% area burrows

Figure 8

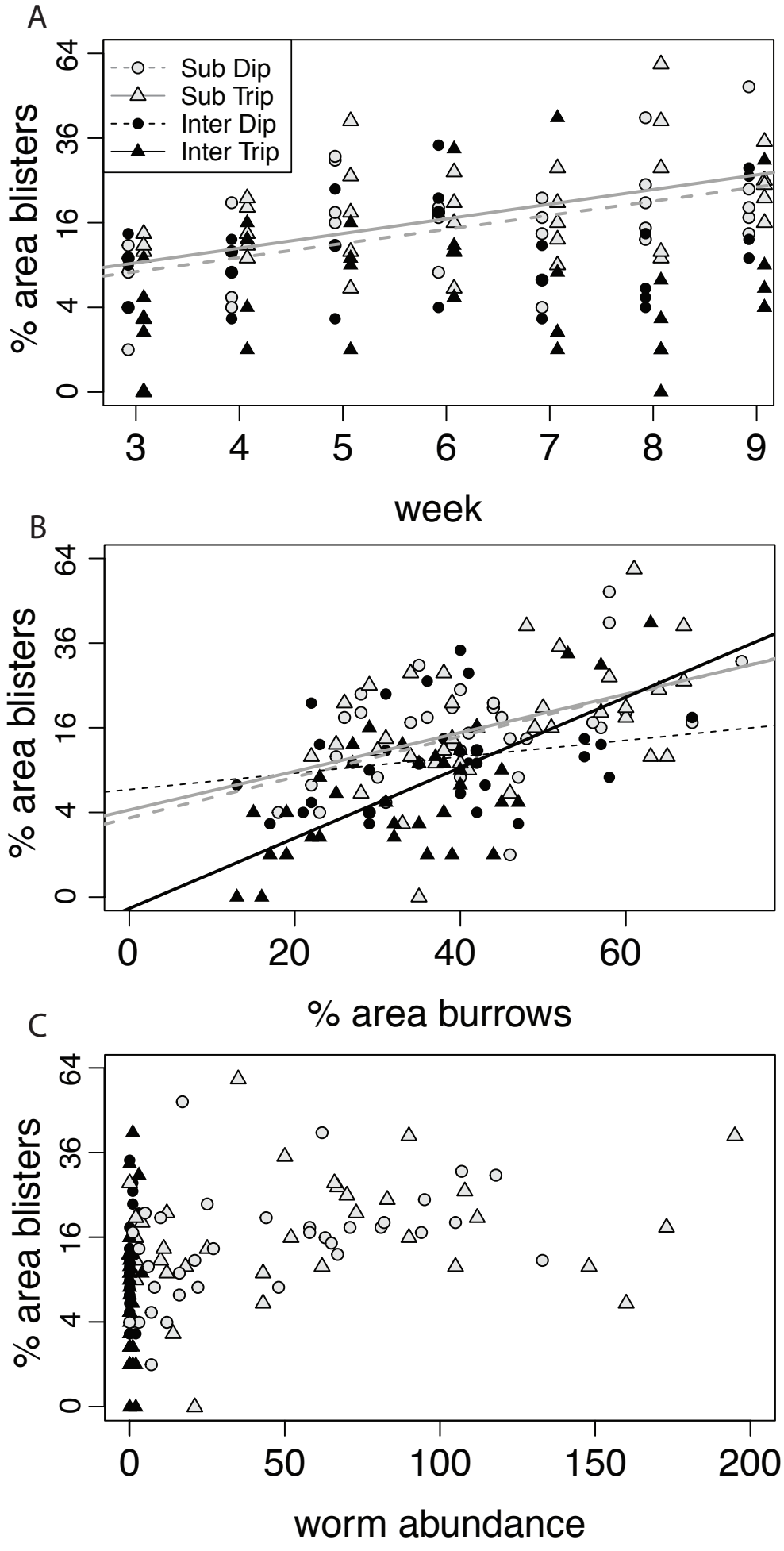
A
Sub Dip
Sub Trip
Inter Dip
Inter Trip
% area blisters
0
4
16
36
64
3
4
5
6
7
8
9
week
B
% area blisters
0
4
16
36
64
0
20
40
60
% area burrows
C
% area blisters
0
4
16
36
64
0
50
100
150
200
worm abundance

Figure A1

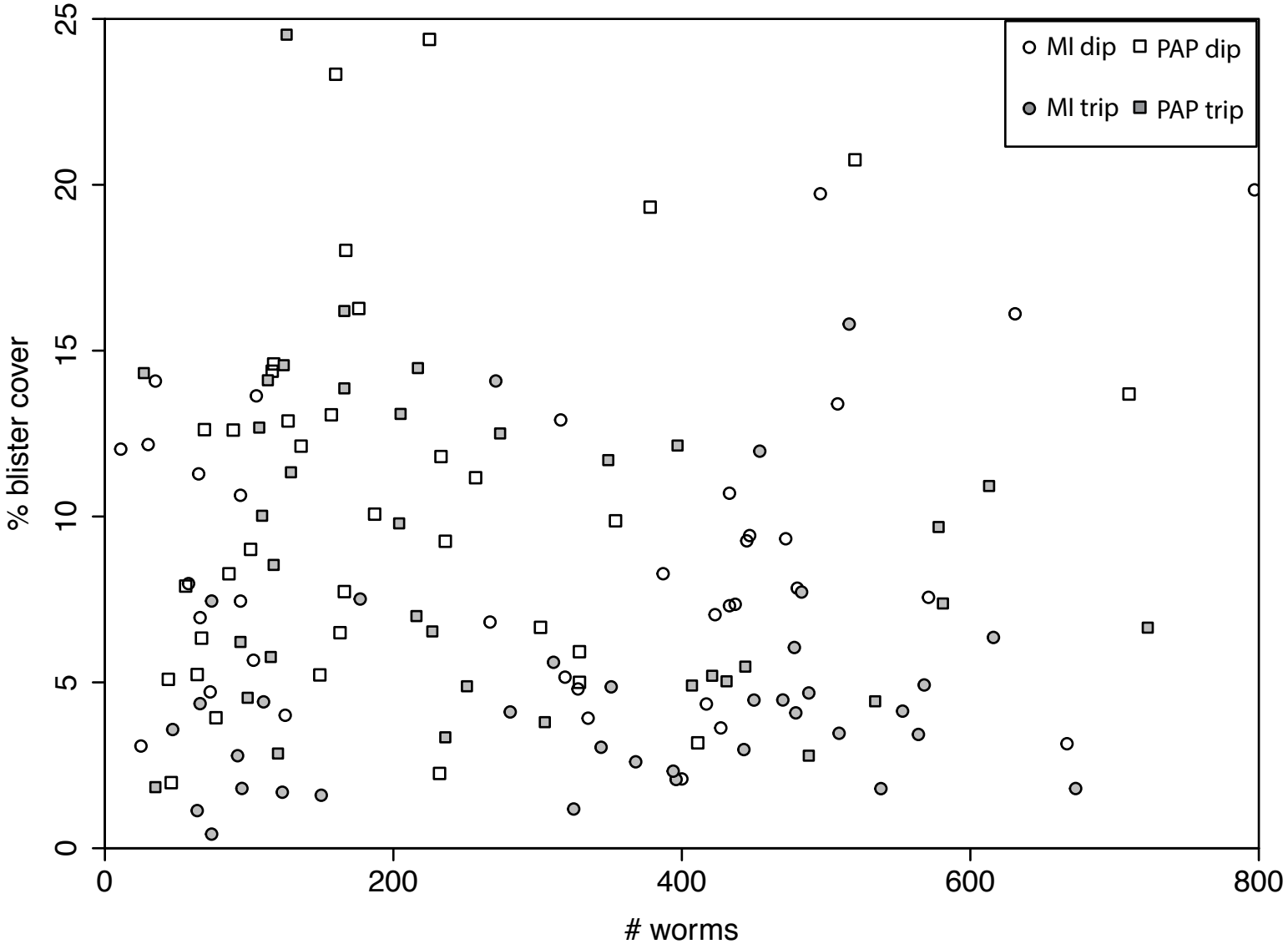
MI dip
PAP dip
MI trip
PAP trip
% blister cover
# worms
0
5
10
15
20
25
0
200
400
600
800

Figure A2

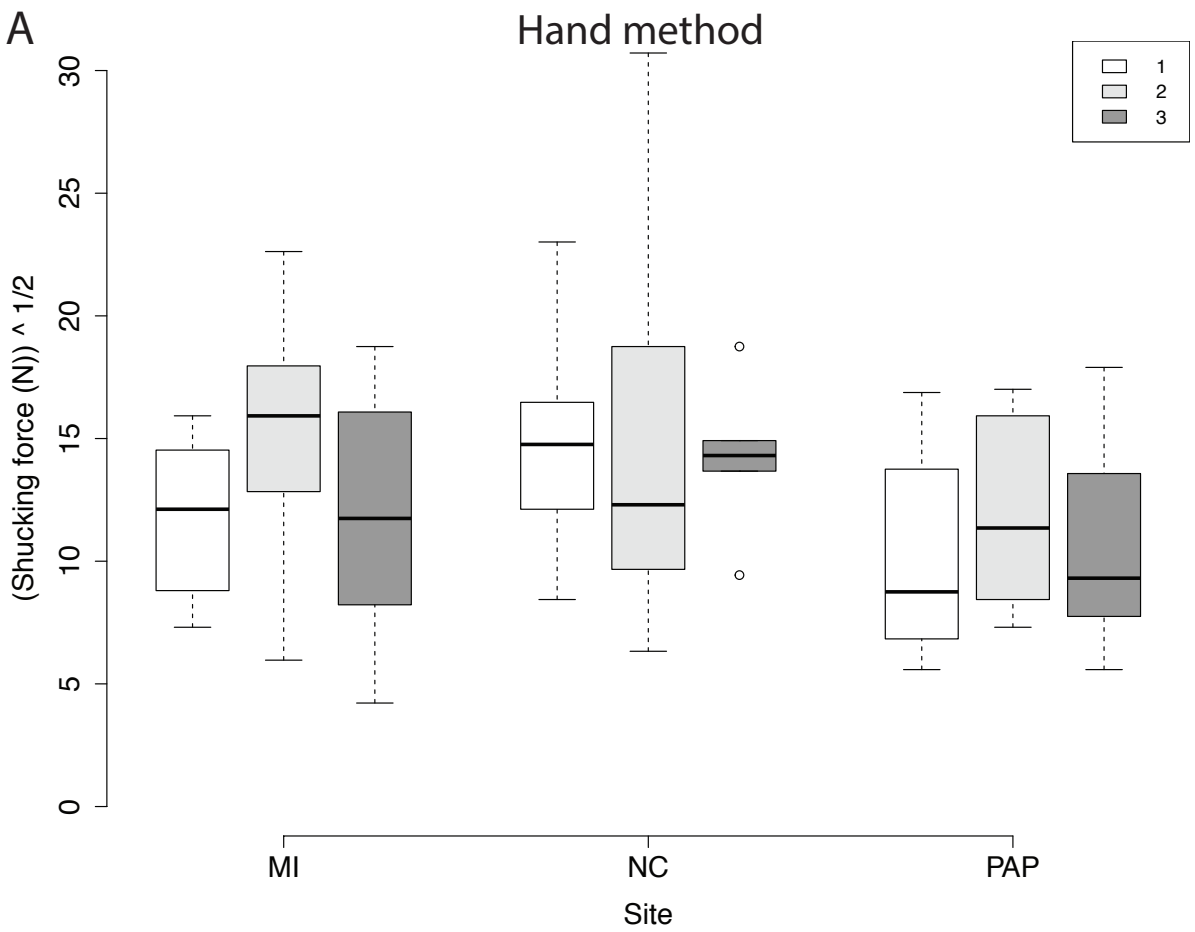
A
Hand method
1
2
3
(Shucking force (N)) ^ 1/2
0
5
10
15
20
25
30
MI
NC
PAP
Site

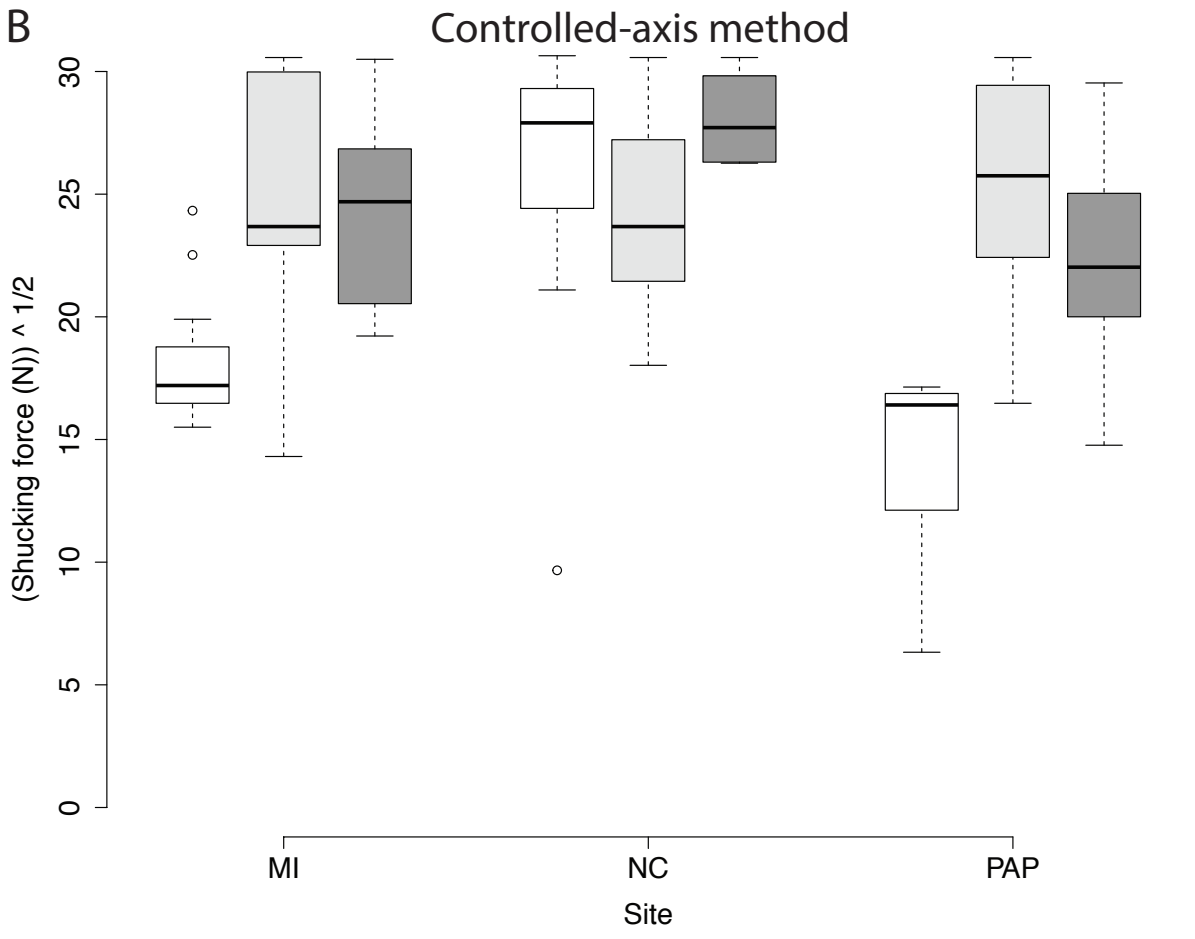
B
Controlled-axis method
(Shucking force (N)) ^ 1/2
0
5
10
15
20
25
30
MI
NC
PAP
Site

Supplementary material: Linear model and linear mixed-effect model result tables

Linear model results Experiment 1 (Fig. 4)

worms extracted (Fig. 4A)

Coefficients: df = 208

	Estimate	Std. Error	t value	Pr(>|t|)	
(Intercept)	2.23681	0.85882	2.605	0.00986	**
Site1	0.06126	1.21871	0.05	0.95996	
Site2	-0.66099	1.2062	-0.548	0.58428	
collection	3.64633	0.26388	13.818	< 2e-16	***
Ploidy	1.06958	0.43139	2.479	1.40E-02	*
Site1:collection	2.74459	0.3738	7.342	4.66E-12	***
Site2:collection	-3.40394	0.37193	-9.152	< 2e-16	***
Site1:Ploidy	0.21201	0.61075	0.347	0.72885	
Site2:Ploidy	-1.17673	0.60872	-1.933	0.05458	.

Navy Cove: null model

Massacre Island

Coefficients :

	Estimate	Std. Error	t value	Pr(>|t|)	
(Intercept)	2.2981	1.7132	1.341	1.84E-01	
collection	6.3909	0.5246	12.184	<2e-16	***
Ploidy	1.2816	0.8566	1.496	0.139	

Point aux Pins

Coefficients :

	Estimate	Std. Error	t value	Pr(>|t|)	
(Intercept)	2.8365	1.7538	1.617	0.1104	
collection	4.3057	0.537	8.018	1.85E-11	***
Ploidy	2.0343	0.8769	2.32	0.0233	*

% shell covered by blisters (Fig. 4B)

Coefficients :

	Estimate	Std. Error	t value	Pr(>|t|)	
(Intercept)	3.81808	0.17564	21.739	< 2e-16	***

Ploidy	-0.87386	0.11123	-7.856	1.99E-13	***
Site1	-0.11849	0.24884	-0.476	0.634433	
Site2	0.45589	0.24748	1.842	0.066862	.
Ploidy:Site1	0.03219	0.15748	0.204	0.838259	
Ploidy:Site2	-0.60865	0.15695	-3.878	0.000141	***

 # blisters

Coefficients:

	Estimate	Std. Error	t value	Pr(>|t|)	
(Intercept)	3.592622	0.177303	20.263	< 2e-16	***
Site1	0.083433	0.25672	0.325	0.7455	
Site2	0.193432	0.24643	0.785	4.33E-01	
Ploidy	-0.482953	0.107596	-4.489	1.19E-05	***
Pw.Extracted	0.005631	0.002307	2.441	0.0155	*
Site1:Ploidy	-0.086916	0.151886	-0.572	0.5678	
Site2:Ploidy	-0.373962	0.151295	-2.472	0.0142	*
Site1:Pw.Extracted	-0.00461	0.002322	-1.985	0.0485	*
Site2:Pw.Extracted	0.009432	0.004594	2.053	0.0413	*

Navy cove

Coefficients: df = 70

	Estimate	Std. Error	t value	Pr(>|t|)	
(Intercept)	3.786054	0.371335	10.196	1.77E-15	***
Ploidy	-0.856915	0.230775	-3.713	0.000408	***
Pw.Extracted	0.015064	0.008619	1.748	0.08491	.

Massacre Island df = 69

Coefficients:

	Estimate	Std. Error	t value	Pr(>|t|)	
(Intercept)	3.6760547	0.2557517	14.374	< 2e-16	***
Ploidy	-0.5698685	0.1476772	-3.859	0.000253	***
Pw.Extracted	0.0010213	0.0003718	2.747	0.007671	**

Point aux Pins

Coefficients: df = 70

	Estimate	Std. Error	t value	Pr(>|t|)	
(Intercept)	3.2858626	0.1424067	23.074	<2e-16	***
Pw.Extracted	0.0007955	0.0004924	1.616	0.111	

Shucking force *ANOVA table presented because of Site differences

Anova Table (Type III tests)

Response: Shucking.ForceT

	Sum Sq	Df	F value	Pr(>F)	
(Intercept)	6458.5	1	266.0621	< 2.2e-16	***
Shucking.Method	172.3	1	7.0997	8.39E-03	**
Site	753.2	2	15.5137	5.91E-07	***
collection	266.6	1	10.9822	0.001107	**
Shucking.Method:collection	210.6	1	8.6771	0.003637	**
Residuals	4490.7	185			

Hand method

Anova Table (Type III tests)

Response: Shucking.ForceT

	Sum Sq	Df	F value	Pr(>F)	
(Intercept)	15036.9	1	642.2797	< 2.2e-16	***
Site	247.5	2	5.2862	0.006751	**
Residuals	2107.1	90			

Controlled axis method

Anova Table (Type III tests)

Response: Shucking.ForceT

	Sum Sq	Df	F value	Pr(>F)	
(Intercept)	4533.4	1	186.4335	< 2.2e-16	***
collection	378.9	1	15.5818	0.0001544	***
Site	353.9	2	7.277	0.0011642	**
collection:Site	111.3	2	2.2881	0.1072073	
Residuals	2237.1	92			

Blister breaking force linear mixed-effect model results (Figure 5).

NAVY COVE

Controlled-axis method Full model

Linear mixed-effects model fit by REML
Data: machineNC
AIC BIC logLik
2294.813 2364.562 -1129.407

Random effects:
Formula: ~1 | Sample.ID
(Intercept) Residual
StdDev: 3.101089 4.4108

Fixed effects: Blister.Breaking.ForceT ~ Color * Blister.Area * Ploidy * collection

	Value	Std.Error	DF	t-value	p-value
(Intercept)	18.34633	3.63795	332	5.043041	0
Color	0.33974	0.66108	332	0.513917	0.6077
Blister.Area	-0.164164	0.156322	332	-1.050165	0.2944
Ploidy1	-4.228459	3.63795	24	-1.162319	0.2565
collection	-1.296007	1.77247	332	-0.731187	0.4652
Color:Blister.Area	-0.007216	0.027737	332	-0.260165	0.7949
Color:Ploidy1	-0.10947	0.66108	332	-0.165593	0.8686
Blister.Area:Ploidy1	0.070627	0.156322	332	0.451806	0.6517
Color:collection	-0.189918	0.325172	332	-0.584053	0.5596
Blister.Area:collection	0.113839	0.08442	332	1.348479	0.1784
Ploidy1:collection	1.698862	1.77247	332	0.958471	0.3385
Color:Blister.Area:Ploidy1	0.018888	0.027737	332	0.68098	0.4964
Color:Blister.Area:collection	-0.001586	0.014742	332	-0.107575	0.9144
Color:Ploidy1:collection	0.000897	0.325172	332	0.00276	0.9978
Blister.Area:Ploidy1:collection	-0.069427	0.08442	332	-0.822395	0.4114
Color:Blister.Area:Ploidy1:collection	-0.005466	0.014742	332	-0.370789	0.711

Controlled-axis method Best Model

Linear mixed-effects model fit by REML
Data: machineNC
AIC BIC logLik
2237.454 2253.119 -1114.727

Random effects:

Formula: ~1 | Sample.ID
(Intercept) Residual
StdDev: 3.403991 4.509582

Fixed effects: Blister.Breaking.ForceT ~ Ploidy

	Value	Std.Error	DF	t-value	p-value
(Intercept)	15.731076	0.744941	347	21.117212	0
Ploidy1	-1.854927	0.744941	24	-2.490032	0.0201

Hand method full model

Linear mixed-effects model fit by REML
Data: handNC
AIC BIC logLik
1012.042 1071.048 -488.021

Random effects:
Formula: ~1 | Sample.ID
(Intercept) Residual
StdDev: 1.754835 1.825199

Fixed effects: Blister.Breaking.ForceT ~ Color * Blister.Area * Ploidy * collection

	Value	Std.Error	DF	t-value	p-value
(Intercept)	10.330391	1.659149	173	6.226319	0
Color	-0.115123	0.2856377	173	-0.40304	0.6874
Blister.Area	-0.074917	0.0582636	173	-1.285829	0.2002
Ploidy1	0.94746	1.659149	23	0.571052	0.5735
collection	-0.672525	0.8040903	173	-0.83638	0.4041
Color:Blister.Area	0.007167	0.0115637	173	0.619804	0.5362
Color:Ploidy1	0.013627	0.2856377	173	0.047706	0.962
Blister.Area:Ploidy1	0.038608	0.0582636	173	0.662644	0.5084
Color:collection	-0.092539	0.1430869	173	-0.646736	0.5187
Blister.Area:collection	0.026386	0.0281496	173	0.937334	0.3499
Ploidy1:collection	0.203016	0.8040903	173	0.252479	0.801
Color:Blister.Area:Ploidy1	-0.003975	0.0115637	173	-0.34378	0.7314
Color:Blister.Area:collection	-0.002256	0.0058357	173	-0.386654	0.6995
Color:Ploidy1:collection	-0.050519	0.1430869	173	-0.353062	0.7245
Blister.Area:Ploidy1:collection	-0.017719	0.0281496	173	-0.629448	0.5299
Color:Blister.Area:Ploidy1:collection	0.001549	0.0058357	173	0.265473	0.791

Hand method best model

Linear mixed-effects model fit by REML
 Data: handNC
     AIC   BIC   logLik
  930.869 944.2574 -461.4345

Random effects:
 Formula: ~1 | Sample.ID
        (Intercept) Residual
StdDev: 2.01876 1.872005

Fixed effects: Blister.Breaking.ForceT ~ Color

	Value	Std.Error	DF	t-value	p-value
(Intercept)	8.369252	0.5909763	186	14.161739	0
Color	-0.243066	0.07733	186	-3.143235	0.0019

MASSACRE ISLAND

MI Controlled axis method Full model

Linear mixed-effects model fit by REML
 Data: machineMI
     AIC   BIC   logLik
  2487.548 2558.136 -1225.774

Random effects:
 Formula: ~1 | Sample.ID
        (Intercept) Residual
StdDev: 2.707555 5.051992

Fixed effects: Blister.Breaking.ForceT ~ Color * Blister.Area * Ploidy * collection

	Value	Std.Error	DF	t-value	p-value
(Intercept)	11.026868	4.289226	356	2.5708291	0.0106
Color	1.361827	0.686166	356	1.9846911	0.0479
Blister.Area	0.082601	0.069145	356	1.1946016	0.233
PloidyTriploid	5.824164	5.778116	17	1.0079693	0.3276
collection	3.747062	2.035103	356	1.8412148	0.0664
Color:Blister.Area	-0.016232	0.011655	356	-1.392689	0.1646
Color:PloidyTriploid	-1.581994	0.942534	356	-1.6784476	0.0941
Blister.Area:PloidyTriploid	-0.06411	0.084283	356	-0.7606486	0.4474
Color:collection	-0.985429	0.338972	356	-2.9071118	0.0039

Blister.Area:collection	-0.066394	0.032975	356	-2.0134519	0.0448
PloidyTriploid:collection	-2.805717	2.649576	356	-1.0589306	0.2903
Color:Blister.Area:PloidyTriploid	0.005855	0.015538	356	0.3768319	0.7065
Color:Blister.Area:collection	0.011138	0.005557	356	2.0041145	0.0458
Color:PloidyTriploid:collection	0.94142	0.448696	356	2.0981275	0.0366
Blister.Area:PloidyTriploid:collection	0.049181	0.038991	356	1.261354	0.208
Color:Blister.Area:PloidyTriploid:collection	-0.006922	0.007093	356	-0.9759319	0.3298

MI Controlled axis method Best model

Linear mixed-effects model fit by REML
 Data: machineMI
      AIC   BIC   logLik
 2418.908 2450.493 -1201.454

Random effects:
 Formula: ~1 | Sample.ID
       (Intercept) Residual
StdDev: 2.67513 5.082914

Fixed effects: Blister.Breaking.ForceT ~ Color + Blister.Area + Ploidy + collection + Ploidy:collection

	Value	Std.Error	DF	t-value	p-value
(Intercept)	21.318481	1.507668	366	14.140037	0
Color	-0.365796	0.1188326	366	-3.078246	0.0022
Blister.Area	-0.01922	0.0036139	366	-5.31832	0
PloidyTriploid	-4.172323	2.0860563	17	-2.000101	0.0617
collection	-1.968911	0.4704356	366	-4.185294	0
PloidyTriploid:collection	2.796623	0.7796242	366	3.587143	0.0004

MI Hand method Full model

Linear mixed-effects model fit by REML
 Data: handMI
      AIC   BIC   logLik
 1796.237 1865.211 -880.1185

Random effects:
 Formula: ~1 | Sample.ID
       (Intercept) Residual

StdDev: 0.8639558 2.465344

Fixed effects: Blister.Breaking.ForceT ~ Color * Blister.Area * Ploidy * collection

	Value	Std.Error	DF	t-value	p-value
(Intercept)	10.191066	1.6676378	321	6.111079	0
Color	-0.676693	0.3174123	321	-2.131905	0.0338
Blister.Area	0.012838	0.0145472	321	0.882521	0.3782
PloidyTriploid	1.587914	2.4023743	20	0.660977	0.5162
collection	-0.682348	0.7075703	321	-0.964353	0.3356
Color:Blister.Area	-0.004021	0.0033072	321	-1.215949	0.2249
Color:PloidyTriploid	0.488989	0.4487153	321	1.089752	0.2766
Blister.Area:PloidyTriploid	-0.011435	0.0362511	321	-0.315451	0.7526
Color:collection	0.237115	0.138329	321	1.714135	0.0875
Blister.Area:collection	-0.009161	0.0065372	321	-1.401419	0.1621
PloidyTriploid:collection	-0.906771	1.0521023	321	-0.861866	0.3894
Color:Blister.Area:PloidyTriploid	0.002132	0.010612	321	0.20095	0.8409
Color:Blister.Area:collection	0.002541	0.0014288	321	1.778329	0.0763
Color:PloidyTriploid:collection	-0.172809	0.2004352	321	-0.86217	0.3892
Blister.Area:PloidyTriploid:collection	0.017225	0.0173583	321	0.992316	0.3218
Color:Blister.Area:PloidyTriploid:collection	-0.003752	0.0048943	321	-0.766529	0.4439

MI Hand method Best Model

Linear mixed-effects model fit by REML
Data: handMI
AIC BIC logLik
1706.806 1737.692 -845.4029

Random effects:
Formula: ~1 | Sample.ID
(Intercept) Residual
StdDev: 0.8842336 2.490522

Fixed effects: Blister.Breaking.ForceT ~ Color + Ploidy + collection + Color:collection + Ploidy:collection

	Value	Std.Error	DF	t-value	p-value
(Intercept)	8.971526	1.0604188	331	8.460361	0
Color	-0.516167	0.1777666	331	-2.903623	0.0039
PloidyTriploid	4.475582	0.9401243	20	4.760627	0.0001
collection	-0.206426	0.4493664	331	-0.459371	0.6463
Color:collection	0.18099	0.0787992	331	2.296846	0.0223

PloidyTriploid:collection	-2.030141	0.38036	331	-5.33742	0

Both methods had significant interactions, so were split by collection date and ploidy for further analysis.

MI Controlled-axis Collection 1 Full model

Linear mixed-effects model fit by REML
Data: machineMI1
AIC BIC logLik
626.6792 652.2179 -303.3396

Random effects:
Formula: ~1 | Sample.ID
(Intercept) Residual
StdDev: 1.537928 3.92158

Fixed effects: Blister.Breaking.ForceT ~ Color * Blister.Area * Ploidy

	Value	Std.Error	DF	t-value	p-value
(Intercept)	21.13883	2.309005	85	9.154954	0
Color	0.006509	0.350866	85	0.01855	0.9852
Blister.Area	-0.008921	0.036506	85	-0.244386	0.8075
PloidyTriploid	-0.758823	3.166972	10	-0.239605	0.8155
Color:Blister.Area	-0.002789	0.006123	85	-0.455553	0.6499
Color:PloidyTriploid	-0.237882	0.492953	85	-0.482566	0.6306
Blister.Area:PloidyTriploid	-0.005047	0.043996	85	-0.114709	0.9089
Color:Blister.Area:PloidyTriploid	-0.000638	0.008051	85	-0.079239	0.937

MI Controlled-axis Collection 1 Best model

Linear mixed-effects model fit by REML
Data: machineMI1
AIC BIC logLik
592.8014 605.8272 -291.4007

Random effects:
Formula: ~1 | Sample.ID
(Intercept) Residual
StdDev: 1.402134 3.873264

Fixed effects: Blister.Breaking.ForceT ~ Blister.Area + Ploidy

	Value	Std.Error	DF	t-value	p-value
(Intercept)	21.305975	0.7976085	90	26.71232	0

Blister.Area	-0.026644	0.0051552	90	-5.16851	0
PloidyTriploid	-2.27964	1.1628146	10	-1.96045	0.0784

Note that here diploids have marginally higher breaking force than triploids (in contrast to hypothesis)

MI Controlled axis Collection 2 full model

Linear mixed-effects model fit by REML
Data: machineMI2
AIC BIC logLik
960.489 990.3934 -470.2445

Random effects:
Formula: ~1 | Sample.ID
(Intercept) Residual
StdDev: 3.097007 4.36708

Fixed effects: Blister.Breaking.ForceT ~ Color * Blister.Area * Ploidy

	Value	Std.Error	DF	t-value	p-value
(Intercept)	13.331765	1.2039298	179	11.07354	0
Color	-0.445893	0.1323475	179	-3.369108	0.0009
Blister.Area	-0.030767	0.0116403	179	-2.643177	0.0089
Ploidy1	1.043324	1.2039298	16	0.866598	0.399
Color:Blister.Area	0.003835	0.0025475	179	1.505434	0.134
Color:Ploidy1	-0.271955	0.1323475	179	-2.054855	0.0413
Blister.Area:Ploidy1	-0.046212	0.0116403	179	-3.970047	0.0001
Color:Blister.Area:Ploidy1	0.007988	0.0025475	179	3.135773	0.002

MI Controlled axis Collection 2 Best model

Linear mixed-effects model fit by REML
Data: machineMI2
AIC BIC logLik
943.9761 965.0505 -464.988

Random effects:
Formula: ~1 | Sample.ID
(Intercept) Residual
StdDev: 3.023572 4.359863

Fixed effects: Blister.Breaking.ForceT ~ Color + Blister.Area + Ploidy + Color:Blister.Area

	Value	Std.Error	DF	t-value	p-value
(Intercept)	13.709987	1.6266941	140	8.428128	0

Color	-0.607652	0.1601867	140	-3.793397	0.0002
Blister.Area	-0.068178	0.0205157	140	-3.323188	0.0011
PloidyTriploid	4.050607	1.903614	10	2.127851	0.0592
Color:Blister.Area	0.010368	0.0035751	140	2.899984	0.0043

MI Controlled axis Collection 3 Full model

Linear mixed-effects model fit by REML
Data: machineMI3
AIC BIC logLik
776.7176 804.8394 -378.3588

Random effects:
Formula: ~1 | Sample.ID
(Intercept) Residual
StdDev: 1.764313 3.784532

Fixed effects: Blister.Breaking.ForceT ~ Color * Blister.Area * Ploidy

	Value	Std.Error	DF	t-value	p-value
(Intercept)	22.213356	2.4637429	114	9.016101	0
Color	-1.122699	0.4123701	114	-2.722552	0.0075
Blister.Area	-0.063479	0.0358085	114	-1.772748	0.0789
PloidyTriploid	-2.195591	3.1332546	9	-0.700738	0.5012
Color:Blister.Area	0.006978	0.005983	114	1.166319	0.2459
Color:PloidyTriploid	0.683158	0.5227281	114	1.306908	0.1939
Blister.Area:PloidyTriploid	0.028786	0.0413939	114	0.695406	0.4882
Color:Blister.Area:PloidyTriploid	-0.003922	0.0074272	114	-0.528116	0.5984

MI Controlled axis Collection 3 Best model

Linear mixed-effects model fit by REML
Data: machineMI3
AIC BIC logLik
747.5061 764.5712 -367.753

Random effects:
Formula: ~1 | Sample.ID
(Intercept) Residual
StdDev: 1.810755 3.764649

Fixed effects: Blister.Breaking.ForceT ~ Color + Blister.Area + Ploidy

	Value	Std.Error	DF	t-value	p-value
(Intercept)	19.106325	1.503348	118	12.709183	0
Color	-0.562763	0.209452	118	-2.686837	0.0083

Blister.Area	-0.022067	0.0059717	118	-3.695213	0.0003
PloidyTriploid	1.665604	1.2988317	9	1.282387	0.2318

MI Hand method Collection 1 Full model

Linear mixed-effects model fit by REML
Data: handMI1
AIC BIC logLik
436.8567 460.2948 -208.4284

Random effects:
Formula: ~1 | Sample.ID
(Intercept) Residual
StdDev: 1.212241 2.14605

Fixed effects: Blister.Breaking.ForceT ~ Color * Blister.Area * Ploidy

	Value	Std.Error	DF	t-value	p-value
(Intercept)	9.236885	1.1226444	67	8.227793	0
Color	-0.234849	0.1998614	67	-1.175061	0.2441
Blister.Area	-0.003751	0.0085443	67	-0.438954	0.6621
PloidyTriploid	1.119599	1.5802486	10	0.708495	0.4948
Color:Blister.Area	0.000067	0.002002	67	0.033461	0.9734
Color:PloidyTriploid	0.036783	0.2867409	67	0.12828	0.8983
Blister.Area:PloidyTriploid	-0.002425	0.0253974	67	-0.095491	0.9242
Color:Blister.Area:PloidyTriploid	0.001301	0.0079585	67	0.163456	0.8707

MI Hand method Collection 1 Best model

Linear mixed-effects model fit by REML
Data: handMI1
AIC BIC logLik
389.8802 401.9138 -189.9401

Random effects:
Formula: ~1 | Sample.ID
(Intercept) Residual
StdDev: 1.209673 2.105957

Fixed effects: Blister.Breaking.ForceT ~ Color + Ploidy

	Value	Std.Error	DF	t-value	p-value
(Intercept)	8.720991	0.7695992	72	11.331862	0
Color	-0.176168	0.1075016	72	-1.638752	0.1056
PloidyTriploid	1.500033	0.8535161	10	1.757475	0.1093

MI Hand method Collection 2 full model

Linear mixed-effects model fit by REML
Data: handMI2
AIC BIC logLik
572.6598 599.0071 -276.3299

Random effects:
Formula: ~1 | Sample.ID
(Intercept) Residual
StdDev: 0.7417327 2.410632

Fixed effects: Blister.Breaking.ForceT ~ Color * Blister.Area * Ploidy

	Value	Std.Error	DF	t-value	p-value
(Intercept)	7.842159	1.2757607	93	6.147046	0
Color	-0.061207	0.1900654	93	-0.32203	0.7482
Blister.Area	0.016063	0.0103909	93	1.545902	0.1255
PloidyTriploid	0.783235	1.8798633	10	0.416644	0.6857
Color:Blister.Area	-0.003416	0.0021765	93	-1.569541	0.1199
Color:PloidyTriploid	-0.027045	0.2665992	93	-0.101446	0.9194
Blister.Area:PloidyTriploid	0.001086	0.0128215	93	0.084723	0.9327
Color:Blister.Area:PloidyTriploid	-0.000564	0.003233	93	-0.174352	0.862

MI Hand method Collection 2 best model

Linear mixed-effects model fit by REML
Data: handMI2
AIC BIC logLik
546.9692 563.0062 -267.4846

Random effects:
Formula: ~1 | Sample.ID
(Intercept) Residual
StdDev: 0.7252436 2.373578

Fixed effects: Blister.Breaking.ForceT ~ Color + Blister.Area + Color:Blister.Area

	Value	Std.Error	DF	t-value	p-value
(Intercept)	8.120084	0.9038609	96	8.983776	0
Color	-0.061193	0.1277442	96	-0.479028	0.633
Blister.Area	0.017037	0.0056524	96	3.014057	0.0033
Color:Blister.Area	-0.003725	0.0013355	96	-2.788931	0.0064

MI Hand method Collection 3 full model

Linear mixed-effects model fit by REML
 Data: handMI3
      AIC   BIC   logLik
 767.9316 798.2359 -373.9658

Random effects:
 Formula: ~1 | Sample.ID
       (Intercept) Residual
StdDev: 2.144362 2.016305

Fixed effects: Blister.Breaking.ForceT ~ Color * Blister.Area * Ploidy

	Value	Std.Error	DF	t-value	p-value
(Intercept)	8.285193	0.8648223	142	9.580226	0
Color	-0.082291	0.1166799	142	-0.705271	0.4818
Blister.Area	-0.002679	0.0119711	142	-0.2238	0.8232
Ploidy1	0.478233	0.8648223	11	0.552984	0.5913
Color:Blister.Area	-0.000596	0.0025907	142	-0.230065	0.8184
Color:Ploidy1	0.00211	0.1166799	142	0.018081	0.9856
Blister.Area:Ploidy1	-0.006589	0.0119711	142	-0.550436	0.5829
Color:Blister.Area:Ploidy1	0.002251	0.0025907	142	0.86895	0.3863

MI Hand method Collection 3 best model
Linear mixed-effects model fit by REML
 Data: handMI3
      AIC   BIC   logLik
 717.5791 729.8547 -354.7896

Random effects:
 Formula: ~1 | Sample.ID
       (Intercept) Residual
StdDev: 2.159265 1.999684

Fixed effects: Blister.Breaking.ForceT ~ Ploidy

	Value	Std.Error	DF	t-value	p-value
(Intercept)	8.305627	0.8474116	148	9.801172	0
PloidyTriploid	-1.243042	1.2484503	11	-0.995668	0.3408

MI Controlled axis Triploids Full Model

Linear mixed-effects model fit by REML
 Data: machineT_MI
      AIC   BIC   logLik

967.5844 997.2825 -473.7922

Random effects:
Formula: ~1 | Sample.ID
(Intercept) Residual
StdDev: 2.392214 4.764165

Fixed effects: Blister.Breaking.ForceT ~ Color * Blister.Area * collection

	Value	Std.Error	DF	t-value	p-value
(Intercept)	16.885699	3.632491	135	4.648518	0
Color	-0.213408	0.607829	135	-0.351099	0.7261
Blister.Area	0.017879	0.045399	135	0.393817	0.6943
collection	0.917315	1.594953	135	0.575136	0.5662
Color:Blister.Area	-0.010229	0.009681	135	-1.056604	0.2926
Color:collection	-0.047114	0.276339	135	-0.170495	0.8649
Blister.Area:collection	-0.017029	0.019606	135	-0.868602	0.3866
Color:Blister.Area:collection	0.004176	0.004154	135	1.005377	0.3165

MI Controlled axis Triploids Best Model

Linear mixed-effects model fit by REML
Data: machineT_MI
AIC BIC logLik
933.2521 951.2354 -460.6261

Random effects:
Formula: ~1 | Sample.ID
(Intercept) Residual
StdDev: 2.297564 4.725695

Fixed effects: Blister.Breaking.ForceT ~ Color + Blister.Area + collection

	Value	Std.Error	DF	t-value	p-value
(Intercept)	17.435709	1.7454152	139	9.989433	0
Color	-0.342696	0.175199	139	-1.956036	0.0525
Blister.Area	-0.024591	0.0059037	139	-4.165314	0.0001
collection	0.726308	0.5761391	139	1.260647	0.2095

MI Controlled axis Diploids Full Model

Linear mixed-effects model fit by REML
Data: machineD_MI
AIC BIC logLik
1522.265 1556.603 -751.1327

Random effects:
Formula: ~1 | Sample.ID
(Intercept) Residual
StdDev: 3.001965 5.221104

Fixed effects: Blister.Breaking.ForceT ~ Color * Blister.Area * collection

	Value	Std.Error	DF	t-value	p-value
(Intercept)	10.979136	4.44907	221	2.467737	0.0144
Color	1.36679	0.709359	221	1.926797	0.0553
Blister.Area	0.081965	0.071539	221	1.145742	0.2531
collection	3.772205	2.104243	221	1.792666	0.0744
Color:Blister.Area	-0.016188	0.012058	221	-1.342528	0.1808
Color:collection	-0.986916	0.35043	221	-2.816299	0.0053
Blister.Area:collection	-0.06606	0.034109	221	-1.936728	0.0541
Color:Blister.Area:collection	0.011107	0.005748	221	1.932366	0.0546

MI Controlled axis Diploids Best Model

Linear mixed-effects model fit by REML
Data: machineD_MI
AIC BIC logLik
1497.47 1521.597 -741.7349

Random effects:
Formula: ~1 | Sample.ID
(Intercept) Residual
StdDev: 3.094655 5.262347

Fixed effects: Blister.Breaking.ForceT ~ Color + Blister.Area + collection + Color:collection

	Value	Std.Error	DF	t-value	p-value
(Intercept)	15.309701	3.399469	224	4.503556	0
Color	0.640533	0.530284	224	1.207905	0.2284
Blister.Area	-0.016129	0.004564	224	-3.534146	0.0005
collection	1.121098	1.582922	224	0.708246	0.4795
Color:collection	-0.530672	0.261934	224	-2.025976	0.044

MI Hand method Triploids Full Model

Linear mixed-effects model fit by REML
Data: handT_MI
AIC BIC logLik
721.2722 751.3117 -350.6361

Random effects:
Formula: ~1 | Sample.ID
(Intercept) Residual
StdDev: 0.4711544 1.93804

Fixed effects: Blister.Breaking.ForceT ~ Color * Blister.Area * collection

	Value	Std.Error	DF	t-value	p-value
(Intercept)	11.697664	1.3292774	139	8.800017	0
Color	-0.182189	0.2468047	139	-0.73819	0.4616
Blister.Area	0.002026	0.0259117	139	0.078177	0.9378
collection	-1.531389	0.5994132	139	-2.554814	0.0117
Color:Blister.Area	-0.002153	0.0078676	139	-0.273635	0.7848
Color:collection	0.062289	0.1128281	139	0.552074	0.5818
Blister.Area:collection	0.007637	0.0125743	139	0.607353	0.5446
Color:Blister.Area:collection	-0.001089	0.0036613	139	-0.297472	0.7666

MI Hand method Triploids Best Model

Linear mixed-effects model fit by REML
Data: handT_MI
AIC BIC logLik
694.7475 715.9147 -340.3738

Random effects:
Formula: ~1 | Sample.ID
(Intercept) Residual
StdDev: 0.4705342 1.928613

Fixed effects: Blister.Breaking.ForceT ~ Color + Blister.Area + collection + Color:Blister.Area

	Value	Std.Error	DF	t-value	p-value
(Intercept)	10.918157	0.6914047	142	15.791267	0
Color	-0.05743	0.0786666	142	-0.730038	0.4666
Blister.Area	0.016076	0.0051698	142	3.109669	0.0023
collection	-1.114875	0.2097978	142	-5.314043	0
Color:Blister.Area	-0.004448	0.0016114	142	-2.760505	0.0065

MI Hand method Diploids Full Model

Linear mixed-effects model fit by REML
Data: handD_MI
AIC BIC logLik

1054.929 1087.504 -517.4645

Random effects:
Formula: ~1 | Sample.ID
(Intercept) Residual
StdDev: 1.174119 2.798917

Fixed effects: Blister.Breaking.ForceT ~ Color * Blister.Area * collection

	Value	Std.Error	DF	t-value	p-value
(Intercept)	10.168496	1.9072751	182	5.331426	0
Color	-0.697633	0.3616224	182	-1.929176	0.0553
Blister.Area	0.012305	0.0165631	182	0.742941	0.4585
collection	-0.651606	0.806067	182	-0.808377	0.4199
Color:Blister.Area	-0.003864	0.0037649	182	-1.02621	0.3062
Color:collection	0.245146	0.1576898	182	1.554611	0.1218
Blister.Area:collection	-0.008877	0.0074377	182	-1.193473	0.2342
Color:Blister.Area:collection	0.002465	0.0016257	182	1.515992	0.1313

MI Hand method Diploids Best Model

Linear mixed-effects model fit by REML
Data: handD_MI
AIC BIC logLik
1008.016 1027.685 -498.0081

Random effects:
Formula: ~1 | Sample.ID
(Intercept) Residual
StdDev: 1.279847 2.791904

Fixed effects: Blister.Breaking.ForceT ~ Color + collection + Color:collection

	Value	Std.Error	DF	t-value	p-value
(Intercept)	10.566092	1.674054	186	6.311679	0
Color	-0.885642	0.3093673	186	-2.862754	0.0047
collection	-1.002821	0.7034376	186	-1.4256	0.1557
Color:collection	0.367384	0.1352245	186	2.716842	0.0072

POINT AUX PINS

PAP Controlled axis method Full model

Linear mixed-effects model fit by REML
Data: machinePAP

AIC BIC logLik
2923.758 2998.811 -1443.879

Random effects:
Formula: ~1 | Sample.ID
(Intercept) Residual
StdDev: 2.053201 4.007206

Fixed effects: Blister.Breaking.ForceT ~ Color * Blister.Area * Ploidy * collection

	Value	Std.Error	DF	t-value	p-value
(Intercept)	15.934195	2.3189713	456	6.871234	0
Color	0.099402	0.3862041	456	0.257383	0.797
Blister.Area	0.055002	0.0386766	456	1.42211	0.1557
Ploidy1	-2.294055	2.3189713	22	-0.989255	0.3333
collection	0.411417	1.0615338	456	0.387568	0.6985
Color:Blister.Area	-0.010123	0.006032	456	-1.678276	0.094
Color:Ploidy1	0.402679	0.3862041	456	1.042659	0.2977
Blister.Area:Ploidy1	0.048225	0.0386766	456	1.246888	0.2131
Color:collection	-0.087222	0.1860119	456	-0.468903	0.6394
Blister.Area:collection	-0.022853	0.0186818	456	-1.223272	0.2219
Ploidy1:collection	0.98006	1.0615338	456	0.923249	0.3564
Color:Blister.Area:Ploidy1	-0.008779	0.006032	456	-1.45545	0.1462
Color:Blister.Area:collection	0.002882	0.0031449	456	0.916401	0.3599
Color:Ploidy1:collection	-0.182346	0.1860119	456	-0.98029	0.3275
Blister.Area:Ploidy1:collection	-0.02582	0.0186818	456	-1.382074	0.1676
Color:Blister.Area:Ploidy1:collection	0.00429	0.0031449	456	1.364033	0.1732

PAP Controlled axis best model

Linear mixed-effects model fit by REML
Data: machinePAP
AIC BIC logLik
2847.192 2863.986 -1419.596

Random effects:
Formula: ~1 | Sample.ID
(Intercept) Residual
StdDev: 1.98184 4.110418

Fixed effects: Blister.Breaking.ForceT ~ Color

	Value	Std.Error	DF	t-value	p-value
(Intercept)	17.441057	0.7031081	469	24.805656	0.00E+00
Color	-0.334796	0.0971026	469	-3.447862	6.00E-04

PAP Hand method Full model

Linear mixed-effects model fit by REML
Data: handPAP
AIC BIC logLik
1979.625 2051.336 -971.8126

Random effects:
Formula: ~1 | Sample.ID
(Intercept) Residual
StdDev: 1.037603 2.188364

Fixed effects: Blister.Breaking.ForceT ~ Color * Blister.Area * Ploidy * collection

	Value	Std.Error	DF	t-value	p-value
(Intercept)	9.625503	1.1704686	375	8.223632	0
Color	-0.17763	0.187269	375	-0.948528	0.3435
Blister.Area	-0.005919	0.0259518	375	-0.228076	0.8197
Ploidy1	1.512798	1.1704686	22	1.292472	0.2096
collection	-0.484902	0.5212801	375	-0.930214	0.3529
Color:Blister.Area	-0.000574	0.0045235	375	-0.126959	0.899
Color:Ploidy1	-0.09489	0.187269	375	-0.506707	0.6127
Blister.Area:Ploidy1	0.009239	0.0259518	375	0.355988	0.722
Color:collection	-0.005506	0.0912058	375	-0.060369	0.9519
Blister.Area:collection	0.003856	0.0125865	375	0.306331	0.7595
Ploidy1:collection	-0.191543	0.5212801	375	-0.367448	0.7135
Color:Blister.Area:Ploidy1	-0.00332	0.0045235	375	-0.734031	0.4634
Color:Blister.Area:collection	-0.000685	0.0024609	375	-0.278549	0.7807
Color:Ploidy1:collection	-0.016649	0.0912058	375	-0.182541	0.8553
Blister.Area:Ploidy1:collection	-0.00982	0.0125865	375	-0.780175	0.4358
Color:Blister.Area:Ploidy1:collection	0.002465	0.0024609	375	1.001561	0.3172

Hand method PAP best model

Linear mixed-effects model fit by REML
Data: handPAP
AIC BIC logLik
1885.84 1901.915 -938.9201

Random effects:
Formula: ~1 | Sample.ID
(Intercept) Residual
StdDev: 1.184117 2.233554

Fixed effects: Blister.Breaking.ForceT ~ Color

	Value	Std.Error	DF	t-value	p-value
(Intercept)	8.342685	0.4188524	388	19.917959	0.00E+00
Color	-0.203698	0.0605325	388	-3.365097	8.00E-04

Hand method PAP alternate model

Linear mixed-effects model fit by REML
Data: handPAP

AIC	BIC	logLik
1891.153	1915.236	-939.5766

Random effects:
Formula: ~1 | Sample.ID

	(Intercept)	Residual
StdDev:	1.176251	2.230762

Fixed effects: Blister.Breaking.ForceT ~ Color * Ploidy

	Value	Std.Error	DF	t-value	p-value
(Intercept)	8.396055	0.4185797	387	20.058438	0
Color	-0.211154	0.060588	387	-3.485084	0.0005
Ploidy1	0.728807	0.4185797	22	1.741143	0.0956
Color:Ploidy1	-0.097473	0.060588	387	-1.608783	0.1085

Linear model results Exp. 2 **(Fig. 7,8)**

Subtidal worm abundance: full

Coefficients: df = 62

	Estimate	Std. Error	t value	Pr(>|t|)	
(Intercept)	-8.3423	4.1207	-2.024	0.04724	*
Week	1.4674	0.6699	2.19	0.03227	*
X.Area.Burrows	31.7183	10.101	3.14	0.00259	**
Ploidy1	3.9118	4.1207	0.949	0.34615	
Week:X.Area.Burrows	-3.0541	1.611	-1.896	0.06266	.
Week:Ploidy1	-0.4188	0.6699	-0.625	0.53414	
X.Area.Burrows:Ploidy1	-9.3839	10.101	-0.929	0.35649	
Week:X.Area.Burrows:Ploidy1	0.9993	1.611	0.62	0.53736	

Subtidal worm abundance: best

Coefficients: df = 66

	Estimate	Std. Error	t value	Pr(>|t|)	
(Intercept)	-8.349	4.036	-2.069	0.0425	*
Week	1.4705	0.6574	2.237	0.02867	*
X.Area.Burrows	32.1198	9.8785	3.251	0.00181	**
Week:X.Area.Burrows	-3.0986	1.5792	-1.962	0.05397	.

BLISTER COVERAGE

Intertidal, all oysters df = 59

	Estimate	Std. Error	t value	Pr(>|t|)	
(Intercept)	0.11363	0.04214	2.696	0.00912	**
X.Area.Burrows	0.51278	0.11211	4.574	2.51E-05	***
Ploidy1	0.14044	0.04214	3.333	0.00149	**
X.Area.Burrows:Ploidy1	-0.31904	0.11211	-2.846	0.00608	**

Intertidal diploids df = 26

	Estimate	Std. Error	t-value	Pr(>|t|)	
(Intercept)	0.25407	0.06274	4.05	0.000411	***
X.Area.Burrows	0.19374	0.15916	1.217	0.234429	

Multiple R-squared: 0.05392, Adjusted R-squared: 0.01753

Intertidal triploids df = 33

	Estimate	Std. Error	t value	Pr(>|t|)	
(Intercept)	-0.02681	0.05638	-0.476	0.638	
X.Area.Burrows	0.83181	0.15806	5.263	8.50E-06	***
	Multiple R-squared: 0.4563, Adjusted R-squared: 0.4398				

Subtidal, all oysters df = 67

	Estimate	Std. Error	t-value	Pr(>|t|)	
(Intercept)	0.041646	0.052628	0.791	0.432	
X.Area.Burrows	0.408633	0.09441	4.328	5.13E-05	***
Week	0.030079	0.006288	4.784	9.83E-06	***